



**UNIVERSITY OF NAIROBI**

**INVESTIGATING THE TELECONNECTION BETWEEN ENSO AND BASIN-SCALE  
FLOODING: CASE STUDY OF NZOIA RIVER BASIN, WESTERN KENYA**

**HEZRON AWITI ANDANG'O**

**I56/87565/2016**

**A RESEARCH DISSERTATION SUBMITTED IN PARTIAL FULFILMENT OF THE  
REQUIREMENTS FOR THE AWARD OF THE DEGREE OF MASTER OF SCIENCE IN  
METEOROLOGY OF THE UNIVERSITY OF NAIROBI**

**NOVEMBER 2023**

## DECLARATION

I hereby declare that this Dissertation is my original work and has not been submitted elsewhere for examination, award of degree or publication. Where other people's work or my own work has been used, this has been properly acknowledged and referenced in accordance with the University of Nairobi's requirements.



Signature

Date: 30/11/2023

Hezron Awiti Andang'o

I56/87565/2016

Department of Earth and Climate Sciences

Faculty of Science and Technology

University of Nairobi

This Dissertation has been submitted with our approval as University supervisors

Signature.....



Date.. 30th November 2023


**Prof. Nzioka J. Muthama**

Department of Earth and Climate Sciences

Faculty of Science and Technology

University of Nairobi

Signature...



Date: November 30, 2023

Prof. Alfred Opere

Department of Earth and Climate Sciences

Faculty of Science and Technology

University of Nairobi

## **DEDICATION**

To my lovely mum, Mrs. Benter Phoebe Andang'o, who instilled in me the spirit of hard work and perseverance and my late dad, Mr. Herbert Ben Andang'o, who I wasn't able to meet and share with as a father.

## **ACKNOWLEDGEMENT**

All gratitude goes to God for taking me through this entire journey.

I wish to sincerely appreciate my two supervisors, Prof. John Nzioka Muthama and Prof. Alfred Opere for the academic mentoring they have inculcated in me. Their astute approach to scientific questions and valuable discussions made working with them not only fulfilling academically, but also enriched my personality.

I wish to also express my gratitude to the Department of Meteorology, University of Nairobi, under Chairmanship of Prof. Franklin Joseph Opijah for the support they accorded me during my entire study period.

Finally, to my beloved family – my lovely mum, my brother and sisters for their enormous backing, moral and relentless support during the course of my study period.

May our Good Lord richly bless you.

## **ABSTRACT**

Even though there is progress in enhancing flood forecasting in Kenya, floods still continue to cause multiple casualties and substantial damages to infrastructure and properties leading to massive economic losses in areas like the Nzoia River Basin within Western Kenya. This unfortunately might worsen in the future, considering factors like climate change, urbanization and increased vulnerability of populations.

The main objective of the study was to establish the teleconnection between ENSO and basin scale floods within the Nzoia River Basin. The datasets used included daily rainfall observations, the Climate Hazards Group InfraRed Precipitation with Station data (CHIRPS), Potential Evapotranspiration (PET), Oceanic Niño Index (ONI) for ENSO analysis, and daily river discharge.

To determine a comprehensive picture of rainfall across the Nzoia Basin, the rainfall data obtained was subjected to spatio-temporal analysis. Analysis entailed an identification of trends or patterns in the rainfall data, such as deviations in the intensity and frequencies of rainfall events over the years.

From the results, there is an increasing trend of precipitation received over the basin from the western to the eastern part as evident from the mean annual precipitation ratio. Also, the basin receives consistently higher mean monthly rainfall from the months of March to May which represents the long rainy season in Kenya.

The relationship between ENSO and daily rainfall within the Nzoia River Basin was determined through statistical analysis using the box and whisker plots. Box and whisker plots would represent the distributions of historical daily rainfall linked to ENSO over the Basin.

To represent the relevant flood simulation processes within the Nzoia River Basin, the GR4J model, a lumped daily model, belonging to Soil Moisture Accounting Model (SMA) group was considered.

ENSO – daily rainfall relationship results showed a greater variability in the extreme daily rainfall response (95<sup>th</sup> Percentile) to strong El Nino events in comparison with the daily rainfall greater than 1mm. Further results also indicated that during some strong El Nino events, slightly less intense rainfall events were experienced within the basin.

Hydrological modelling simulations showed that the observed and simulated flows have a similar pattern with rainfall variability over the basin except for a small bias that could be ascribed to either the response time of the catchment to extreme rainfall events especially during the ENSO years.

The GR4J model showed a better performance with the Nash-Sutcliffe criterion (NSE) outcome values indicating an acceptable performance of above 50% both during the calibration and validation period. Even though there was a difference amongst the calibration and validation phases, the GR4J acquires higher performance during the calibration phase hence could be efficient to perform and reproduce high river flows in the basin.

The study findings enhance the existing knowledge on ENSO impacts on extreme rainfall and flooding and provide a foundation for routine provision of sub-seasonal to seasonal flood forecasts. This, in the long run is expected to contribute considerably to a better management and sustainable growth of socio-economic activities which have been greatly impacted by floods over the years.

## TABLE OF CONTENTS

DECLARATION .....	ii
DEDICATION .....	iii
ACKNOWLEDGEMENT .....	iv
ABSTRACT.....	v
TABLE OF CONTENTS.....	vii
LIST OF TABLES .....	x
LIST OF FIGURES .....	xi
LIST OF ACRONYMS AND ABBREVIATIONS .....	xii
CHAPTER ONE .....	1
INTRODUCTION .....	1
1.1 Background .....	1
1.2 Problem statement .....	3
1.3 Research questions .....	4
1.4 Objectives.....	4
1.5 Hypothesis.....	4
1.6 Justification and Significance of the study.....	5
1.6.1 Impact Based Action Approach .....	6
1.7 Study area.....	7
1.7.1 Domain and Physical Features of the Study Area .....	7
1.7.2 Climatology of the study area .....	8
CHAPTER TWO .....	10
2 LITERATURE REVIEW .....	10
2.1 Introduction .....	10
2.2 Spatial-temporal characteristics of Western Kenya’s rainfall.....	10
2.3 The El Niño-Southern Oscillation (ENSO).....	11
2.3.1 Main Features.....	11
2.3.2 ENSO Impacts and Teleconnections .....	12
2.4 Other large-scale drivers of Rainfall in Western Kenya .....	14
2.4.1 Inter-Tropical Convergence Zone (ITCZ) .....	14

2.4.2	Indian Ocean Dipole (IOD) .....	15
2.4.3	Madden-Julian Oscillation (MJO) .....	16
2.4.4	Tropical Cyclones .....	17
2.4.5	The Quasi-Biennial Oscillation (QBO) .....	17
2.4.6	East African Low Level Jet (EALLJ) .....	18
2.4.7	Sub-Tropical Anticyclones .....	19
2.4.8	Monsoons .....	20
2.5	Causes and Impacts of Floods in Kenya .....	20
2.6	Flood Modelling .....	23
2.6.1	Introduction to Hydrological Models .....	23
2.6.2	GR4J Model .....	24
2.7	Conceptual Framework .....	26
CHAPTER THREE .....		28
3 DATA AND METHODOLOGY .....		28
3.1	Introduction .....	28
3.2	Data .....	28
3.2.1	Rainfall Observations .....	28
3.2.2	Climate Hazards Group InfraRed Precipitation with Station data (CHIRPS) .....	29
3.2.3	Potential Evapotranspiration (PET) .....	29
3.2.4	ENSO Indices .....	30
3.2.5	Daily River discharge observations .....	30
3.3	Methodology .....	30
3.3.1	Time Series Analysis .....	30
3.3.2	Spatial-temporal Analysis .....	30
3.3.3	Box and whisker plots .....	32
3.3.4	Significance Tests .....	33
3.3.4.1	Monte Carlo Simulation/Resampling .....	33
3.3.5	GR4J Model Calibration/Validation .....	34
CHAPTER FOUR .....		36
4 RESULTS AND DISCUSSIONS .....		36
4.1	Validation of CHIRPS .....	36



4.2	Objective 1 - Spatial and Temporal Rainfall Distribution .....	37
4.2.1	Spatial Distribution .....	37
4.2.1.1	Annual and Seasonal Rainfall Distribution.....	38
4.2.1.2	Mean Annual and Seasonal Rainfall variability.....	40
4.2.1.3	Annual and Seasonal Precipitation ratio .....	41
4.2.2	Temporal Distribution of Daily Rainfall.....	42
4.2.3	Spatial Distribution of Potential evapotranspiration.....	43
4.2.4	Temporal Variation of Potential evapotranspiration.....	44
4.3	Objective 2 - ENSO effect on Rainfall Distribution .....	45
4.3.1	Rainfall distribution greater than 1mm .....	46
4.3.2	Extreme daily rainfall distribution (95 <sup>th</sup> Percentile) .....	49
	The red dashed lines represent the 5 <sup>th</sup> and 95 <sup>th</sup> percentiles while the blue continuous line represent the Monte Carlo median.....	53
4.4	Objective 3 - Hydrological Modelling Results .....	54
4.4.1	GR4J Model Performance.....	56
	CHAPTER FIVE .....	60
	5 SUMMARY, CONCLUSIONS AND RECOMMENDATIONS .....	60
5.1	Summary .....	60
5.2	Conclusions .....	61
5.3	Recommendations .....	61
5.3.1	Research Scientists and Research Institutions .....	61
5.3.2	Policy makers.....	62
5.3.3	Users of Climate/Flooding/Modeling Information: .....	62
	REFERENCES .....	63

## LIST OF TABLES

Table 1: List of stations and coordinates used in the study .....	28
Table 2: Table of Pearson correlation (r) between observed and Chirps data .....	37
Table 3: Annual and Seasonal Rainfall Distribution summary for Nzoia River Basin .....	38
Table 4: Annual and Seasonal Rainfall Precipitation Ratios for Nzoia Basin.....	38
Table 5: El Nino Years Considered for the study .....	46
Table 6: GR4J Model parameters setting.....	54
Table 7: GR4J Calibration/Validation sub periods.....	54
Table 8: Applied metrics results for the GR4J model.....	55
Table 9: Summary of the statistical characteristics of the basin observations.....	56

## LIST OF FIGURES

Figure 1: Nzoia River basin map and associated river network (green). Source: Othieno, 2022...	8
Figure 2: GR4J model diagram (Perrin et al., 2003).....	25
Figure 3: The conceptual framework of the study (Source: Author).....	27
Figure 4: Comparison between CHIRPS and station(observed) rainfall data . The x-axis represents the time period in months .....	36
Figure 5: (a) Mean Annual Rainfall and (b Seasonal (OND Season) Rainfall Distribution.....	39
Figure 6: (a) Mean Annual Precipitation Ratio and (b) Seasonal (OND) Precipitation Ratio .....	40
Figure 7: Mean Annual Precipitation Ratio (a) and OND (Seasonal) Precipitation Ratio .....	41
Figure 8: Monthly Rainfall Distribution with the Nzoia Basin .....	42
Figure 9: Mean Annual Potential Evapotranspiration (a) and Seasonal (OND) Distribution (b). 43	
Figure 10: Temporal Variation of the Spatial Average of the Potential Evapotranspiration in Nzoia Basin.....	44
Figure 11: Mean Annual Potential Evapotranspiration (a) and Seasonal (OND) Distribution (b). The Red and Blue dashed lines represent thresholds for strong El Nino and La Nina respectively .....	45
Figure 12: Box and whisker plots of daily rainfall greater than 1mm for the whole dataset (blue box) and strong El Nino years (green boxes).....	48
Figure 13: Box and whisker plots of daily rainfall above 95 <sup>th</sup> Percentile the whole dataset (blue box) and strong El Nino years (green boxes).....	50
Figure 14: Significance test results for Bungoma station from Monte Carlo Simulations for daily rainfall above 95 <sup>th</sup> Percentile. ....	52
Figure 15: Significance test results for Bungoma station from Monte Carlo Simulations for daily rainfall above 95 <sup>th</sup> Percentile. ....	53
Figure 16: Rainfall variability, observed and simulated flow rates in calibration (1981-2006) with the GR4J model from the criterion of (NSE (Q)) .....	58
Figure 17: Rainfall variability, observed and simulated flow rates in validation (2007-2021) with the GR4J model from the criterion of (NSE (Q)) .....	59

## LIST OF ACRONYMS AND ABBREVIATIONS

CHIRPS - Climate Hazards Group InfraRed Precipitation with Station data

COADS - Comprehensive Ocean-Atmosphere Data Set

EWS – Early Warning Systems

ENSO - El Niño-Southern Oscillation

FEWSNET - Famine Early Warning Systems Network (FEWS NET)

GCM - General Circulation Model

GHA - Greater Horn of Africa

GDP – Gross Domestic Product

GR4J - *Génie Rural à 4 paramètres Journalier*

HadISST - Hadley Centre global Sea Surface Temperature dataset

ICAPC - IGAD Climate Prediction and Applications Centre

IOD – Indian Ocean dipole

ONI - Oceanic Niño Index

ITCZ - Inter-Tropical Convergence Zone

IPCC – Intergovernmental Panel on Climate Change

JJAS – June July August September Rainfall Season

MAM - March April May Rainfall Season

MJO - Madden-Julian oscillation

NMHS – National Meteorological and Hydrological Services

NOAA - National Oceanic and Atmospheric Administration

OND – October November December Rainfall Season

PET – Potential Evapotranspiration

SST - Sea Surface Temperature

USAID - United States Agency for International Development

WMO - World Meteorological Organization

# CHAPTER ONE

## INTRODUCTION

### 1.1 Background

Floods are costly natural and short-lived events and can normally happen suddenly, occasionally with little or no warning (Gannon et al., 2018; D. A. Macleod et al., 2021; D. Macleod & Caminade, 2019) and commonly as a result of intense storms which enhance river run-offs than the normal channel or infiltration capacity. Floods normally occur as a result of an overflow in stream and river discharges and can cause massive destruction to property and loss of life.

Compared to droughts which normally have slow onsets, the onset of floods is always rapid and result from excess rainfall. Even though the occurrence of floods is random, weather and climate patterns have a major influence. (Bates et al., 2010; Neumann et al., 2018). Other factors including land management practices also contribute to the heightening of land surface run-offs, contributing to river discharges and hence flooding.

The East Africa's and Kenya's rainfall patterns shows significant variability both in space and time. This variability has been found to be a result of major interactions among several processes occurring in different timescales (Aming et al., 2014; Philip Omondi et al., 2013). Areas to the north of the region including parts of Uganda receives most rainfall between June and September. On the other hand, the central regions mostly bordering the equator have two main rainfall seasons; a main one occurring between March and May and a fairly shorter one from October to December.

Major flooding events have affected the region greatly with the last decade due changes in the climate system (Otieno & Anyah, 2013; Serdeczny et al., 2016). Previous scientific studies like (Sciences, 2013; Shongwe et al., 2011; Stevenson et al., 2012; Tierney et al., 2015) have established that a combination of the effects of global warming and climate change have caused an intensification of the global hydrological cycle with changes in extreme rainfall characteristics like durations and frequencies. One of the major characteristic of the East African rainfall pattern is strong seasonal cycle with clearly distinct wet season within a better part of the region. (Tierney

et al., 2015). During the main rainfall season, drier periods normally compromise the accessibility of water available for farming activities and rain fed agriculture which a better percentage of the people normally relies on.

The intraseasonal and interannual rainfall variability over the region is controlled by several remote forcing. Within the October to December rainfall season, there exist a large year to year variability on interannual time scales and strong spatial consistency of rainfall pattern across most parts of the region, which has been linked to circulation anomalies within the tropical Oceans (Nicholson, 2017). Findings from previous studies indicates that during the main rainfall season, East African region experiences varying spatial variability which is weakly linked to global sea surface temperature anomalies (Endris et al., 2019; Shongwe et al., 2011; Stevenson et al., 2012). Recent observations indicate that there have been more frequent droughts within a better part of the East Africa even though the total amount received has reduced during the main rainfall seasons (Chris Funk et al., 2008; Verdin et al., 2005).

El Niño-Southern Oscillation remains a significant recurring occurrence which is one of the oceanic and atmospheric distribution of climate with a periodicity of about 8 years (Lau et al., 2008; Trenberth, 1997). The ENSO phenomena has two extreme phases; a warm phase or 'El Nino' which denotes the warming within the Central or Eastern Pacific Ocean and 'La Niña', a cold phase which refers to the cooling within the Eastern or Central Pacific Ocean. Between these two extreme cases, is another phase referred to as ENSO 'Neutral'. During the ENSO neutral phase, the SSTs within the Nino 4 region is always closer to normal. (Yan et al., 2013).

ENSO signals have been captured in several global parameters including large scale convection, pressure, precipitation, cyclone activities tropospheric temperatures, monsoonal circulations as well as with non-climatic indicators like economic and biological consequences linking it to rainfall anomalies globally. (Hong et al., 2001).

Findings from (Ambrosino et al., 2011; Bahaga et al., 2015; Diro et al., 2011; Philip Omondi et al., 2013) have also associated rainfall extremes over several parts of Africa including Eastern, Southern and Equatorial Africa to the ENSO phenomena. According to Omondi et al. 2013 and

Endris et al. 2019, significant teleconnections exists between ENSO and rainfall patterns within East Africa particularly throughout the Autumn and Summer seasons of the Northern Hemisphere with a robust association being evident along the coastal areas of Kenya during the autumn season.

## **1.2 Problem statement**

Floods remains one of the major extreme events that threaten people's livelihoods and lives within the Sub-Saharan Africa mostly because of great exposure and susceptibility of people. Even though there are currently early warning systems (EWS) in place, they have remained insufficient leading to increased impacts to people and properties. Kenya in particular has been susceptible and harshly affected by impacts of floods and climate variability owing to high seasonality and variations in the inter-annual rainfall (Conway et al., 2005; Schreck & Semazzi, 2004). Additionally, this vulnerability has further been worsened by low income levels among the general population that are exposed. (Beyene et al., 2010).

Heavy rains still continue to have major societal impacts with rising societal impacts. This has led to loss of livelihoods and associated economic losses. Increased knowledge and understanding of the onset, magnitude and duration of the different phases of ENSO can provide a foundation for routine provision of sub-seasonal to seasonal forecasts and associated information and services for regions impacted by ENSO.

Inadequate lead time for flood forecasts still remains a challenge. Further research is therefore needed to enhance the accuracy of long term flood forecasts allowing for better preparedness and response. According to (Joshua et al., 2014), the current flood forecasting models are not flexible for probabilistic or longer lead time forecasting. Another major challenge for Nzoia River Basin is a weak understanding of the major climate divers including ENSO. An expansion of such knowledge would therefore be vital in the operational monitoring and early warning of flood events, as well as formulating anticipation and mitigation procedures which are very fundamental when prioritizing the use of available resources for disaster response.



### **1.3 Research questions**

The following research questions were explored to achieve the study objectives.

1. How is the distribution and characteristics of rainfall over Western Kenya in space and time?
2. How do ENSO impact daily rainfall in Western Kenya?
3. How is the linkage between flooding and extreme rainfall within the Nzoia River Basin during the ENSO years?

### **1.4 Objectives**

The main objective of the study was to establish the teleconnection between ENSO and basin scale floods within the Nzoia River Basin. The following specific objectives were explored to achieve this main objective;

- a) To examine the space-time characteristics of rainfall over Western Kenya during ENSO years.
- b) To investigate the linkages between strong ENSO variations and intraseasonal rainfall during the OND rainfall season over Western Kenya.
- c) To examine the teleconnection between ENSO and flooding in over the Nzoia River Basin.

### **1.5 Hypothesis**

For objective one and two, the hypothesis is that the distribution of the rainfall patterns within the basin is affected by both spatial and temporal factors. Spatially, this could be attributed to the topography and land use characteristics within the basin. Temporally, weather patterns and climate variability can influence the frequency, intensity, and duration of rainfall events. Through analysis of spatiotemporal patterns of rainfall data, a better understanding of the underlying factors that contribute to rainfall variability within the basin could be determined.

For the third objective, the hypothesis for the study is that there exists a teleconnection between ENSO and basin-scale floods within the Nzoia River Basin, whereby warmer sea surface

temperatures associated with El Niño modes results in increased rainfall and hence flooding in downstream basins.

El Niño events are always linked to be warmer-than-normal SSTs within the equatorial Pacific, which can impact weather patterns around the world. Previous research has suggested that ENSO may be linked to basin-scale floods, which occur in large river basins and can have significant socio-economic and environmental impacts. This hypothesis proposes that the mechanism behind this relationship is a teleconnection, whereby atmospheric and oceanic conditions in the Pacific Ocean influence rainfall patterns in downstream basins, leading to increased flood risk. Precisely, in El Niño years enhanced warming in the Pacific causes changes in atmospheric circulation patterns that cause more rainfall to fall in certain areas, potentially leading to increased runoff and flooding in downstream river basins. To test this hypothesis, the following research questions will be answered.

## **1.6 Justification and Significance of the study**

The livelihoods and economies of countries within East Africa is reliant on agriculture which is normally rain fed and greatly sensitive to weather and climatic conditions. Extreme climatic conditions including floods have also been found to greatly affect agriculture in the region leading to low food productivity. (Kandji et al. 2006, Waithaka et al. 2013). Previous studies like Olila and Wasonga 2016, have unfortunately shown that climate variability within the region that is currently being observed is anticipated to increase owing to climate change effects. The subsequent effects of such changes will include adverse effects on food security situation in the region which might lead to other climate and food security related conflicts. Reports by AfDB 2014, Jane Kabubo-Mariara and Kabara 2015 also indicates that climate extremes, variability and change continues to pose significant danger to food security despite progress that have been made in the region.

According to Macleod et al., 2021 and Wainwright et al., 2020, the floods of 2018 in Kenya highlighted the potential impacts of unmatched climatic risks. Addressing these risks is consequently critical and efforts should be focused on building resilience among the most vulnerable populations. Studies from Bizimana, Bessler Regents, and Angerer 2016 also mounts to the fact that various climatic extremes including floods and droughts have increased over the recent years in frequency and intensity within the Eastern Africa region including Kenya.

Several studies have highlighted the teleconnection between various climate drivers and East Africa and Kenya's rainfall variability. Precisely, ENSO is considered among the major drivers of interannual climate variability within the tropics. Previous studies like (Giannini, 2010; Giannini et al., 2008; Plisnier et al., 2000) have linked ENSO to noticeable effects on interannual rainfall variability over East Africa and specifically Kenya.

Based on these previous research findings, one of the best approaches of identifying best policies to support the most exposed in areas affected by these extremes is to understand the forces that control the monthly or seasonal weather and climate patterns. The study will document past and current climate trends, identify main patterns of variability and determine how these patterns align with flooding trends in West Kenya region. This will help determine in advance the likely impacts of these events on livelihoods hence reliable information can appraise the most susceptible and further and plan interventions.

Building upon the existing knowledge of the influence of ENSO, the results generated from this study will also contribute towards a better understanding of the atmospheric circulations over Western Kenya and East Africa as a whole. The findings will provide a crucial information needed for monitoring and early warning of extreme events in Western Kenya.

### **1.6.1 Impact Based Action Approach**

In spite of the constant progress flood forecasting in Kenya, floods still continue to cause multiple casualties and substantial damage to infrastructure and properties yearly leading to massive economic losses for flood prone areas like the Nzoia Basin in Western Kenya. This trend unfortunately might worsen in the future, considering factors like climate change, urbanization, increased exposure and vulnerability of populations. Studies by the European Environment Agency has shown that annual floods have caused major losses and the same will likely rise to fivefold by 2050 and up to 17-fold by 2080. For improvement of Early Warning Systems (EWSs) of extreme rainfall and floods, a shift is needed from hazard to impact forecasting.

Seldom, both meteorological and hydrological forecasts are linked to quantifiable estimates of their potential impacts. As a result, actions from institutions in charge of emergency preparedness/response are grounded on the knowledge accrued by the scientists/forecasters from computer analysis. This, on the other hand makes the decisions to safeguard population and assets to be determined through a personal perception of local risk conditions. Hence, in as much as there is an understanding of what is likely to happen in terms of weather, what the weather might do still remains a challenge. (World Meteorological Organization (WMO), 2021)

For an improvement of the Early Warning Systems, transitioning from a hazard to impact forecasts is necessary. Impact-Based Flood forecasting is a methodology that focuses on providing accurate and timely information on the potential impacts of flooding affecting communities and infrastructure, in addition to traditional flood hazard information such as water levels and flow rates. The impact based approach emphasizes the importance of providing information on potential impacts of a flood, which enables stakeholders to take appropriate action in a timely manner, reducing loss of life and destruction of property. By focusing on impacts, rather than solely on hazard, the approach can help ensure that emergency response resources are deployed more effectively and efficiently.

## **1.7 Study area**

### **1.7.1 Domain and Physical Features of the Study Area**

The Nzoia River Basin (Figure 1) lies between longitude 34°-36°E and latitude 0°03'-1°15' N in Western Kenya. The river is approximately 334km long and drains into Lake Victoria, the biggest freshwater lakes in Kenya. The Nzoia River basin is one of the largest river basins in Kenya and has an approximate area of 12,900km<sup>2</sup>. The basin lies within an altitude range of between 1100 to 3000m (Othieno, 2022) with areas around the Mt. Elgon and Cherangani Hills serving as the main river sources.

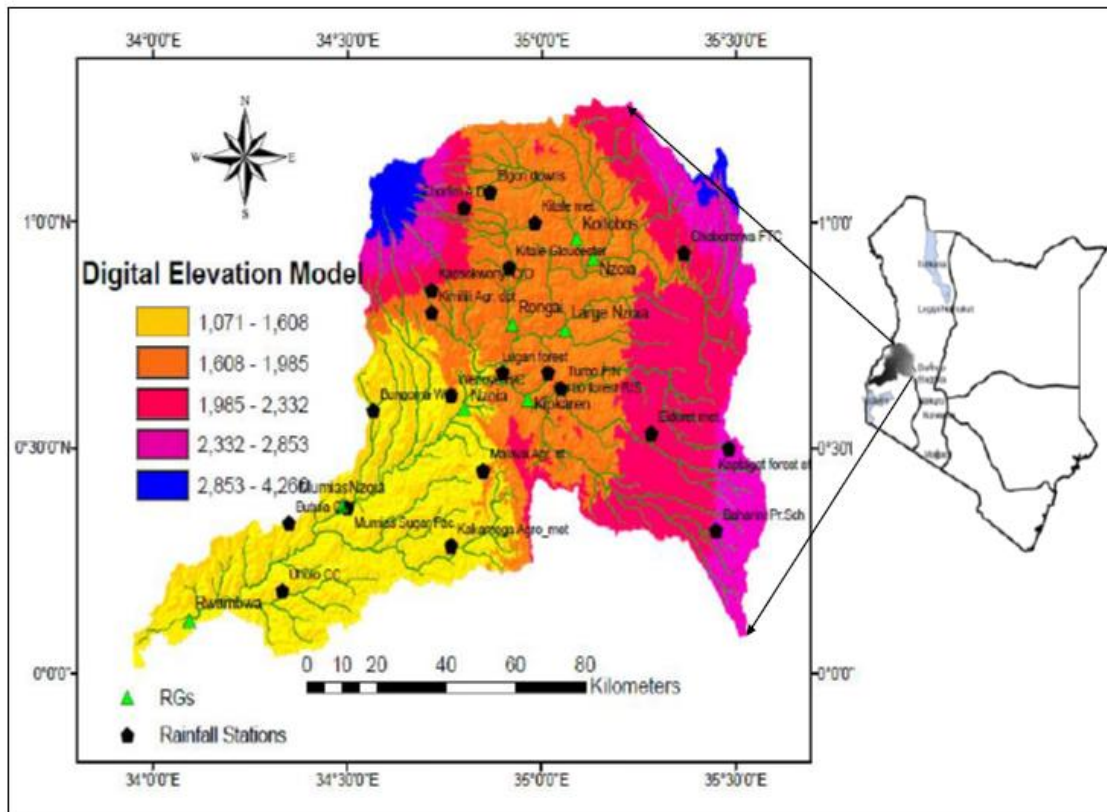


Figure 1: Nzoia River basin map and associated river network (green). Source: Othieno, 2022

### 1.7.2 Climatology of the study area

The Nzoia River Basin generally experiences two rainfall seasons, a long rainfall season from March to May, with a shorter one from October to December. rainfall throughout the year, with a maximum in the month of April. (Omondi et al., 2014). It is important to note that the, for long rains, onset always vary between the start of March to end of April over the basin.

The Nzoia River Basin's climate is typically tropical humid with daily temperatures ranging between 16°C to 28°C within the highland regions of and lowers areas respectively.(Othieno, 2022). The basin's economy is mostly rural-based small scale farming with nearly 90 per cent of the population earning a living from keeping livestock and subsistence agriculture.(Joshua et al., 2014). The lower areas of the basin is generally flat, swampy and flood prone is characterized by mainly clay soils. Most of the farmlands are individually owned with food crops like maize, beans, groundnuts, sorghum, cassava, potatoes, millet and bananas grown (Notification et al., 2006).

The Nzoia River plays a great economic value both to the locals and a country as whole especially in sectors like agriculture, transport, fishing and tourism. The basin has been considered for this study because of its great local and regional importance and majorly because been prone to flooding.

## CHAPTER TWO

### 2 LITERATURE REVIEW

#### 2.1 Introduction

The existing literature on Rainfall characteristics within the Nzoia Basin, ENSO, and flooding in Western Kenya is reviewed in this section.

#### 2.2 Spatial-temporal characteristics of Western Kenya's rainfall

The climate of East Africa shows major a spatial heterogeneity because of great topographical disparities over the region. Within the region, rainfall peaks occur during the boreal spring and autumn with an equatorial rainfall regime prevailing. The boreal spring rains normally occurs between March to May with the autumn one in the October-November period.(B. O. Ayugi et al., 2018; C. Funk et al., 2014) Previous studies like Vigaud, Lyon, and Giannini 2017 indicates an annual rainfall bimodal pattern over a better part of the region with the local climate distribution being linked mostly to the latitudinal movement of the ITCZ. The ITCZ pattern predominantly modifies the South East and North East trade winds during the Northern and Southern summer respectively, resulting into two main rainfall seasons from March to May normally called 'long rains' with a shorter one occurring as of October to December. (Lyon, 2014; Philip Omondi et al., 2013).

With most of the agricultural activities being rain fed, a better part of the East Africa and Kenya's population in particular remains vulnerable to weather and climate variations hence making the country greatly food insecure.(Shukla et al., 2014). This has been worsened by occasionally both rainfall seasons (Lyon & Dewitt, 2012) resulting in major droughts and humanitarian crisis affecting millions of people across the country.

Kenya is specifically located within the Indian and West African monsoons border with rainfall regimes in the bordering Ethiopia and South Sudan being closely associated with the West African monsoon (Nicholson, 2017). Also, both the northeasterly and easterly flows that occurs between

November and March associated with the Indian monsoon has also been found to be linked to the West African monsoon.(Endris et al., 2019)

Western Kenya's general rainfall pattern has been found to be heterogeneous, owing to the intricacy of both large and small scale drivers (Aming et al., 2014). Some of these drivers include water bodies like lakes and maritime influence, topography and dynamics of seasonal variations of circulations within the tropics. Even though the rainfall amount received varies seasonally and greatly over short distances, there is relatively a strong consistency in the inter-annual variability patterns.(Endris et al. 2019, Funk et al. 2014).

Due to ITCZ passage, the Nzoia River Basin also has two rainfall seasons every year. However, there are also influences of local features like Lake Victoria that alter the normal distribution, occasionally leading to a rainfall peak between the main seasons.(Odwori & Wakhungu, 2021). The annual mean rainfall received within most parts the region ranges between 800 and 1200 mm (Cattani et al., 2018; Mutai & Ward, 2000; Nicholson, 2017) but is much higher over highland areas and reduces much over lower areas.

## **2.3 The El Niño-Southern Oscillation (ENSO)**

### **2.3.1 Main Features**

ENSO is a significant climate variability which occurs when sea surface temperatures and pressure are high and low respectively across the Equatorial Pacific. The East Africa and Kenya in specific is among the areas where the impacts of ENSO have been experienced in terms of both temperature and rainfall anomalies.

(Wang et al., 2017) describes it as stable mode mainly triggered by the forcing of stochastic or mode of naturally self-sustained oscillation coupled by the system of the ocean – atmosphere. According to (Lehodey et al., 2021), it is currently known as one of the largest world's fluctuations in natural climate.

ENSO's two main features - El Niño and Southern Oscillation (ENSO) are mainly two diverse occurrences with similar and closely connected characteristics (Gannon et al., 2018). Wang et al., 2017 describes Southern Oscillation as one that is categorized by the inter-annual sea level pressure fluctuation in the tropics between the Western and Eastern Pacific which comprises of a



strengthening and the slackening of the easterly trade winds over the tropical Pacific. (Kim et al., 2021) states that the Southern Oscillation is an air pressure fluctuation in large scale and its negative phase occurs in the El Niño periods and positive in the La Niña periods.

El Niño-Southern Oscillation (ENSO) is considered a major driver of climate variability on an inter-annual timescale with different theories used in its description including the linear stochastic theory.

### **2.3.2 ENSO Impacts and Teleconnections**

Several studies have done to understand the teleconnection between rainfall and climate drivers within the East African region. Chris Funk et al. 2008 for instance associated the positive SST trends within Central and South Indian Ocean to negative trend in rainfall anomalies and modification of regional moisture and wind patterns.

Williams and Funk 2011 linked drier conditions within the region to higher SST gradients within the Indian and Pacific region. However, studies by Lyon & Dewitt, 2012 provided a linkage between the drier conditions to variations SSTs in the tropical Pacific basin coupled with strengthening in Western Pacific. Previous studies to understand the East Africa's seasonal rainfall variations have also associated the same to variations in sea surface temperatures within the southwest Indian Ocean (Cai et al., 2014, 2015; Wang et al., 2019). Ogallo, Janowiak and Halpert 1988; Indeje and Semazzi 2000 among other researchers also studied the linkage between the SST over Pacific and inter-annual variability of rainfall over East Africa.

Both Goddard and Mason 2002 and Goddard and Graham 1999 have shown that wind anomalies at low levels which occurs during El Niño or La Niña years results in the warming or cooling within the Western Indian Ocean zonal SST gradient which is anomalous usually occurs across the Indian Ocean basin causing enhancement or reduction of rainfall to the far east and is enhanced/reduced in the east and on the other hand reduction or increase over East Africa region in the west.

Several studies have also acknowledged the recent reduction in the long rains since 1998 or 1999 to date (Endris et al., 2019, Lyon and Dewitt 2012 and Pricope et al. 2013 ). Other studies have

provided further indication that the East Africa long rains abruptly shifted through the tropical Pacific SST forcing ((Liebmann et al., 2017; Lyon, 2014; Lyon & Dewitt, 2012) while recent trend in warming of the Pacific warm pool has been linked with strong Walker circulation, largely driven by tropical Pacific SST gradient (Bahaga et al., 2015; Cai et al., 2014, 2015; Diro et al., 2011; Enfield & Mestas-nuñez, 2010).

However, with less information well-known at intraseasonal scales there still remains a need for an improvement in knowledge gaps for understanding the rainfall variability and various atmospheric processes. A couple of studies like Berhane and Zaitchik 2014 and Shongwe et al. 2011 depicts an existence of a sub-seasonal connection between the MJO and the variability of the East African long rains. This variability operates through several mechanisms including the Somali low-level jet modulation.

Previous studies by Ogallo, Janowiak, and Halpert 1988 have linked extreme rainfall anomalies over equatorial, eastern and Africa to ENSO. Important teleconnections between the seasonal rainfall over several regions of East Africa and southern oscillation, particularly in the seasons of northern hemisphere autumn and summer were observed by this study. Also (Ogallo, Janowiak, and Halpert 1988) showed that strongest relationships occurred during the autumn season along the coast of Kenya with evidence of a relationship between austral summer rainfall anomalies and cold and warm ENSO phases.

Mutemi et al., 2007 found a strong connection the evolutionary ENSO phase and the rainfall within East Africa, with his findings indicating that ENSO mainly plays major role in the determination of the monthly and seasonal patterns of rainfall in the East African region. (Mutemi 2003) also observed shifts in the onset and cessations of patterns of rainfall over certain region with a reduction that is significant in seasonal peak being evident in others.

Funk et al. 2014 showed that a change in the SST gradients could lead to the strengthening of the Walker circulation branch within the Indian Ocean which may in turn enhance subsidence on East Africa.

According to Korecha and Barnston 2007 and Diro, Grimes, and Black 2011, the main driver of East African rainfall variability during the JJAS season has been linked to the linked to the tropical

seas surface temperatures and ENSO. Overall, the East African interannual rainfall variability have been linked to these SSTs and IOD.

Nonetheless, these past findings have not yet entirely proven the interannual rainfall and ENSO linkages specifically in Kenya. Broad questions proposed in this study will offer further insights into the key above-mentioned climate linkages. Furthermore, this study will lay a foundation for improvement of the existing statistical prediction models for Kenya's rainfall on intraseasonal scales, by ascertaining significant thermodynamic and dynamic oceanic and atmospheric variables.

## **2.4 Other large-scale drivers of Rainfall in Western Kenya**

The distribution of rainfall in Kenya is influenced by several large scale drivers. These systems range from local scale to global scale as well as local physical features. Their interactions normally in complex ways brings about the observed distribution of rainfall in Kenya. These systems include mesoscale systems (for example, land, lake and sea breezes), synoptic scale systems like the tropical cyclones, subtropical quasi-permanent anticyclones (Mascarene, St. Hellena, Arabian, and Azores), global teleconnections with global climatic anomalies like El Nino Southern Oscillation (ENSO), dipole modes like the Indian Ocean Dipole (IOD), Madden-Julian Oscillations (MJO), Quasi-biennial Oscillations (QBO), jet streams, monsoons and easterly waves. The subsequent sections offer brief descriptions of how these systems affect the Kenyan climate.

### **2.4.1 Inter-Tropical Convergence Zone (ITCZ)**

The Inter Tropical Convergence Zone is a fine area which normally forms around the equator where North westerly and South Easterly winds converge. (Byrne & Schneider, 2016). According to Liu et al., 2020 the formation of the ITCZ is normally responsible for over 30 percent of the global precipitation with variability affecting most people living within the tropical regions. ITCZ has also been found to be strongly associated with the Hadley cell atmospheric circulation where it reflects both thermodynamic and dynamic tropical coupling and interactions between the air and the sea over oceans (Xiang et al., 2018).

According to Mukabana, 1992 and Mutai et al., 1998, the ITCZ is the dominant rainfall feature in the region characterized by mass convergence at low level with intensified precipitation that encircles the equatorial region.

Following the seasonal insolation cycle, ITCZ moves across the equator north and southwards and it is closely associated with the seasonal monsoon circulations (Byrne & Schneider, 2016). This movement is one of the prominent patterns in the prediction of shifts in the large scale drivers of precipitation as depicted by global climate models in relative to the climate change response.

The oscillation of the ITCZ over East Africa reaches extreme positions over eastern Africa during July at 15°N and January at 15°S. This oscillation is portrayed in the bimodal nature of rainfall in the larger equatorial east Africa. Suzuki, 2011 showed that the ITCZ is characterized by deep convection, zonal moisture convergence and that its seasonal variability is because of solar insolation changes.

Over East Africa, Okoola, 1999 identified that the ITCZ is influenced by the vigor of the sub-tropical highs. Okoola, 1999 identifies that the onset and cessation of the March to May rains within East Africa is closely associated with the modification of the Inter Tropical Convergence Zone by active convection in the regions of Madagascar (Arabian Sea). Also, the incursions of moisture into the Madagascar region during the long rains create oscillations of active convection between parts of the Indian Ocean and Central Africa.

#### **2.4.2 Indian Ocean Dipole (IOD)**

The Indian Ocean Dipole is a natural kind of variation in climate which occurs mainly due to the oceanic and atmospheric coupled interactions within the Indian ocean and is linked to several variations in the atmospheric state within the Equatorial Indian Ocean on inter-annual time scales. (Hameed et al., 2018). Yuan et al., 2018 highlights IOD's significant global impacts with predominantly severe consequences in the areas around the Indian Ocean basin. Studies by Ummenhofer et al., 2009 has also linked IOD's variability to some of the worst droughts in Australia. Cai et al., 2012 also stated that a positive IOD event increases the threats of fire within the some regions in Australia during the following austral summer season. According to Anderson et al., 2019, there has also been associations of couple of Indian Ocean Dipole events to an increase in food security risks by affecting crop yields. From the same study and Hashizume et al., 2012, other associated risks from this climate mode within the East Africa region includes flooding and disease outbreaks.

Study by Abram et al., 2020 have shown that a negative IOD event comprises the intensification of the zonal sea surface temperature gradients with warming up and cooling in the East and West respectively. Although the negative IOD are generally weaker than positive IOD events they still have caused significant impacts. For instance, the most potent negative IOD event on record which happened in 2016 led to heavy rainfall within the Australia and Indonesia region while enhancing extreme drought in Eastern Africa. (Lim et al., 2017).

### **2.4.3 Madden-Julian Oscillation (MJO)**

The Madden-Julian Oscillation (MJO) comprises of a wave of tropical convection which oscillates from East to West round the globe orbiting through the equator. (Madden & Julian, 1971). The Madden-Julian Oscillation, can be identified in analysis of atmospheric variables since it has unique signatures of zonal wind, temperature and pressure anomalies. The MJO convection has a period in the range of 30-60 days and the average speed is about 5m/s.

The monitoring and detection of MJO events is based on the criteria put forward by Waliser et al., 2009 as follows: - Persistence of OLR anomalies for at least four pentads whereby the zonal existence of the anomaly must exceed 30 degrees of longitude; OLR at the centre should be almost  $-15 \text{ W/m}^2$  and the strongest events should have a minimum 50 degrees' longitude wide and  $-25 \text{ W/m}^2$ . This classification is useful for diagnostic studies and as well for monitoring active weather systems. The most widely used index for MJO propagation monitoring was developed by Wheeler & Hendon, 2004. The index commonly known as the Real-time Multivariate MJO index was founded on a pair of principal component time series.

In Kenya, the Madden-Julian Oscillation has been attributed to the variation in the intra-seasonal rainfall during both the March to May Season and the October to December rains. (Pohl & Camberlin, 2006). In the long rainfall season of MAM, Sandjon et al., 2014 identified that the convection in the region  $70/80^\circ\text{E}$  and  $120^\circ\text{W}$  greatly influence variability of the early March and late May rainfall. This shows that the MJO has the possibility of influencing the seasonal length of rainfall in the region. The MJO signal however has not been detected during April.

Studies by Pohl & Camberlin, 2006 also concurs that the MJO influences the variability of the MAM rainfall by triggering early onsets of the season as well as the occurrence of significant wet

events at the beginning of the season. For October – December season, the MJO strengthens at 120°E (10°W) and has been linked to the occurrences of dry (wet) spells confined only to the East African coast. However, the effects of the system are variable from year to year. According to Omeny et al., 2008, the MJO can also be used to proficiently forecast the intra-seasonal rainfall variability over some regions within East Africa.

#### **2.4.4 Tropical Cyclones**

Tropical cyclones are defined as low pressure centres in the tropics that are characterized by rainfall and strong winds of at least 32m/s that is approximately 64knots. Tropical cyclones can also be referred to as typhoon or hurricanes (P. J. Klotzbach & Oliver, 2015)

According to Klotzbach et al., 2019 tropical cyclones are among the most destructive natural catastrophes that causes many fatalities and damage globally every year. The losses associated with the tropical cyclone from 1971 to 2016 are about \$700billion according to Zsótér et al., 2016 and in 2017 the losses were around \$284.7 billion (CRED, 2019).

Tropical cyclones that modulate the weather in Kenya normally occurs within the South Western Indian Ocean (SWIO). The effects of these systems normally depends on the season, basin of formation and the prevailing synoptic flows (Ongoma et al., 2015). The conditions favorable for their formation include SSTs of at least 26.5°C, reduced vertical wind shear and moisture availability. For this reason, the formation of the cyclones is usually enhanced during active MJO phase over the Indian Ocean.(Ash & Matyas, 2012; P. J. Klotzbach & Oliver, 2015)

#### **2.4.5 The Quasi-Biennial Oscillation (QBO)**

Quasi-Biennial Oscillation is a lower stratospheric circulation involving changes in the phase of zonal winds where we have easterlies for one year and westerlies for another year. The development of the QBO normally starts in the top lower troposphere spreading downwards at an approximate rate of around 1.2km per month. However, this pattern decays upon reaching the lower tropopause (Pascoe et al., 2005).

A couple of studies have linked the occurrence and distribution of rainfall within East Africa to the Quasi-Biennial Oscillation patterns. Ogallo et al., 1988 and Omondi et al., 2012 identified a

2.5-3.7-year rainfall patterns which shows the influence on the QBO on the regional rainfall. The lower stratospheric flow has also shown that extremely excess (deficient) rainfall is associated with easterly (westerly) wind phases (Ng'ongolo & Smyshlyayev, 2010). The findings of this study based on regression techniques, showed that the QBO phase usually for the months preceding the March to May season is suitable for rainfall prediction. Indeje & Semazzi, 2000 found that MAM and JJA rainfall can be forecasted up to a lead time of four months based on the QBO.

#### **2.4.6 East African Low Level Jet (EALLJ)**

A jet stream is a fine horizontal current of air characterized by strong vertical and horizontal wind shear and featuring several velocity maxima in the world. The East African Low Level Jet is southerly low level jet originating from the southern Indian Ocean and is mainly responsible for moisture transport during the Indian summer monsoon. The jet can be observed at 850mb wind vector (Subrahmanyam, 2014). According to (Oscar et al., 2022) the EALLJ forms as a result of cross-equatorial northerly advection of planetary vorticity that is directed to the east coast of Africa by the north-south barrier highlands of East Africa.

The East African highlands are understood as key in restraining the westward advance of the jet, thereby promoting the eastward flow upon crossing the equator. The discovery of this flow is credited to the work of Findlater, 1977. The path of the jet over the lowlands of Kenya, Ethiopia and Somalia is associated with high wind speeds. The diffluent nature of the jet yields dry conditions in the region, save for the coastal zones (Camberlin et al., 2010).

The East African Low Level Jet normally originates within the South West Indian Ocean with associated development to the intensification of the Indian Ocean Anticyclone during the southern hemisphere winter. The jet being diffluent at low levels, it thus does not bring precipitation over the East African region. However, it is responsible for moisture transport into the summer monsoonal region of India.

#### **2.4.7 Sub-Tropical Anticyclones**

East Africa is influenced by both continental and maritime anticyclones. The anticyclones are normally synoptic and near permanent high pressure cells which affects the wind flow and hence moisture and temperature in the region. Their existence is characterized by regions of large scale subsidence located in the borderline of Ferrel and Hadley cells (Tyson et al., 1996).

The Arabian and Azores Highs normally exist in the Northern Hemisphere while the St. Helena and Mascarene High occur in the Southern hemisphere. Due to pressure differences, north (south) hemisphere highs control the flow of the north (south) easterlies. The convergence of these two hemispheric flows generally determines the location of the ITCZ. The highs intensify (weaken) during the respective winter (summer) seasons.

In modulating the wind patterns, the anticyclones normally affect the transport of moist air from the Indian Ocean into Kenya. For other regions like the Atlantic Ocean, the St. Helena high has an influence in promoting the influx of moisture into western Uganda, western Kenya and Tanzania during the JJA season leading to rainfall. The enhancement of both the Mascarene and the St. Helena highs have also been associated with increased rainfall events in East Africa. The Mascarene high can be identified at lower troposphere and migrates within the latitudes 30 - 35°S (Manatsa et al., 2014). The Mascarene high, which drives the south easterlies over a longer trajectory over the Indian Ocean results to intense moisture influx into the region thereby responsible for the long rains during MAM. The anomalous zonal displacement of the Mascarene High has great influence on the variability of the OND rainfall over East Africa. With the displacements to the west (east), the heat and moisture field of the South Indian Ocean is modified resulting to suppressed (enhanced) convective activity over the western Indian Ocean and thereby increasing the likelihood of depressed (enhanced) rainfall over East Africa (Manatsa et al., 2014).

The Arabian high is responsible for the north easterly flow. However, the north easterlies have little moisture due to their short transverse over the ocean and thereby their influence results to the short rains during OND. The dynamics of these anticyclones; position, orientation and intensity as well influence the characteristics of the ITCZ. The Azores high usually modulates the northward



boundary of the West African ITCZ. However, declining trends of rainfall over Kenya, Tanzania and Ethiopia have been associated with the strengthening of the Azores high.

#### **2.4.8 Monsoons**

Monsoons are moist circulations of summer that provide many countries with the most annual rainfall in both the subtropics and the tropics therefore influencing more than a third of the population of the world (Geen et al., 2020). They are also dominant features of the climate of tropical and subtropical in most of the world's regions and they are associated with prevailing winds being seasonally reversed, summer seasons that are rainy and winter seasons being drier. Like the other divers already discussed above, the coastal currents driven by the monsoon winds have been found to have an effect on the circulation of water around the coastal East Africa. (Kamau et al., 2020).

Monsoons are normally formed from the cross- equatorial pressure gradient development which is produced by various physical properties of associated land, ocean and atmospheric systems like differential heating. Through such processes, heat that is normally stored by the oceans and land is transported vertically and modified through differential heating by moist processes,

#### **2.5 Causes and Impacts of Floods in Kenya**

Floods have been a part of Kenya's history since ancient times. Kenya has experienced several notable floods throughout its history. Some significant flood events in Kenya are the 1961 Tana River floods which was caused by heavy rainfall along the Tana River in eastern Kenya, The El Niño weather phenomenon in 1997/1998 which brought heavy rainfall and widespread flooding to various parts of Kenya, 2006 Kenya experienced heavy rains that led to flooding in different regions such as Nairobi, Nyanza, Rift Valley, and Coast provinces, the period between 2010 and 2011 saw heavy rainfall and flooding in different parts of Kenya like Nairobi, Rift Valley, Coast, and Nyanza and 2018, Kenya experienced heavy rainfall that triggered floods in various areas, including Nairobi and western Kenya.

Flooding in Kenya arises from various factors and circumstances and the causes can be attributed to various factors, including meteorological, geographical, and human-induced factors.

Meteorologically, heavy and prolonged rainfall is a primary trigger for flooding. The country normally has two rainfall seasons – a long season occurring between March and May, and a shorter season from October to December. Both seasons are characterized by intense precipitation, overwhelming the natural drainage systems. Kenya's geographical features, such as its proximity to the equator, extensive river systems, lakes and steep terrain, exacerbate the impact of heavy rainfall by rapidly channeling water into vulnerable areas. (Kilavi et al., 2018 )

Okaka and Odhiambo, 2018 stated that both climatic and non-climatic factors have played a role in past and future flooding in Kenya. The El Niño phenomenon, largely influenced by global warming, normally contributes to a higher flood frequency throughout the entire country. The 1997/98 El Niño event is a good example of the devastating floods it can cause. Seasonal rainfall anomalies in East Africa are influenced by SSTs anomalies in the Indian Ocean, particularly when they coincide with El Niño events, as seen in 1997/98. The response of the Indian Ocean temperature to tropical Pacific fluctuations occurs with a few months' time lag. The massive flooding experienced in Kenya during the 1997/98 El Niño phenomenon serves as a notable example.

Even though floods are affected by climate patterns, the drainage basin characteristics and land use both in the upper and downstream including construction of dams and reservoirs influence flooding within a basin. In urban areas, the vulnerability to flood hazards and risks can be attributed to both natural and man-made factors. (Olang & Fürst, 2011)

Recently in 2021, the country has experienced significant flooding events over a better part of the country. (Wanzala, Ficchi, et al., 2022) Data from the Emergency Events Database reveals the country has experienced big flooding events averagely once every two years, with more than 70,000 people being affected per event (B. Ayugi et al., n.d.). According to B. Ayugi et al., n.d., the country has experienced 17 major flood occasions between 1964–2004 with high impact events occurring in 1961, 1997–1998, 2006, 2012, and 2018.

Even though there are benefits of heavy rainfall and flooding including replacement of surface and groundwater resources, enhanced crop yields and livestock fodder among others, losses from the

big events have been massive, ranging from water system damages, infrastructure and communication systems and water borne diseases (Gannon et al., 2018) with have affected millions of people across the country. Gannon et al., 2018 for instance, the flooding events of the 1997/1998 El Nino costed at least USD \$870 million, nearly corresponding to 10% of Kenya's GDP. Averagely, Kenya experiences a flooding event costing around 5.5% of the country's GDP every seven years.

From previous studies including Kilavi et al., 2018 found out that most flooding events in the country occur during the March to May season (long Rains). However, major large-scale climate drivers like ENSO that control weather and climate variability are more active during the OND rainfall season. Even though there are initiatives to enhance forecasts of extreme rainfall and flooding in the flood prone areas including Western Kenya, limited understanding of major climate drivers still exists. An increased understanding of the teleconnection of ENSO and flooding in Western Kenya will enhance forecasts skills and co-production of products over longer lead times and integration into Early Warning System using an Impact Based Action Approach.

According to Owuor & Mwiturubani, 2022, floods can occur in certain river basins even under normal rainfall conditions. This occurrence is mainly attributed to the excessive runoff of surface water caused by unfavorable land practices, such as deforestation, degradation of land upstream, and inadequate cultivation methods.

Talha et al., 2019 found out that most of the floods that induce loses socio-economically are mainly exacerbated by the unabated upsurge in population, development in the urban area, indiscriminate land use and systems that are unregulated in the municipal systems hence it is therefore important to implement a system for the prediction of flood than can potentially be helpful in the consequences of the flood that are induced.

Tempest et al., 2017 indicates that floods have both effects on mental and physical health and it has been associated with the increase in the majority of the effects of the mental health such as the anxiety, post-traumatic stress disorder and depression which can persist several months and years afterwards.

In Kenya, the vulnerability of infrastructure to floods is a cause for concern since in the recent years, the country has encountered major floods episodes that led to high occurrences of most failure in the infrastructure hence leading to losses that are socio-economically associated with the interference with the infrastructural services like the damages of the road networks, social facilities, buildings and even energy facilities (Njogu, 2021). Study done by the Kenya Institute for Public Policy Research and Analysis (KIPPRA) revealed that the floods episodes of 2017 and 2018 in Kenya that occurred in 27 counties had a wide range of effects on user's infrastructure across the different counties.

Flooding disrupts the environmental balance and often creates a favorable environment (breeding grounds) for the proliferation of pathogens and vectors. According to (Brown and Murray, 2013), diseases that are most susceptible to flooding are those that rely on waterborne transmission between hosts or require a host/vector for their life cycle therefore flooding can impede access to and delivery of urgent medical services, leading to further spread of infectious diseases.

## **2.6 Flood Modelling**

Flood modeling is the method of using advanced mathematical and computational techniques to simulate and predict the behavior and consequences of floods in a particular region. It involves analyzing the intricate relationships between various factors like rainfall, water runoff, river channels, floodplains, and more, to understand how flooding occurs and its impact on the area.

Part of the focus for the study will be to model basin scale flooding within the basin. Nzoia River Basin is a medium sized and has been selected for this study because it's among the main basins that are susceptible to flooding the country. The basin also benefits from long and high quality daily discharge datasets.

### **2.6.1 Introduction to Hydrological Models**

Hydrological models are beneficial in both short and medium scale flood predictability (Alfieri et al., 2013; Emerton et al., 2018), risk and hazard mapping, climate and water resource assessment among other uses. (Krysanova et al., 2017). Hydrological variables including stream flow are predicted by hydrological models of different types and which require different input parameters.

In circumstances where few input data exist, these models can always also be used to estimate river flow and runoff within ungauged catchments. (Parajka et al., 2013).

According to (Paul et al., 2020), hydrological model selection for research and or operational flood monitoring and forecasting is not easy due to the representation of different processes, availability of input data, minimization of uncertainties and errors within the modeling chain.

From (Melsen et al., 2019), the choice of model for any application at times becomes difficult because of several reasons including;

- (i) Most hydrological models are not custom-made to particular climate or conditions. This elimination of various processes at times challenging.
- (ii) Similarity in the characteristics and weaknesses of various hydrological models.
- (iii) Generally, there is a lack of a classification to rank models and ascertain appropriateness
- (iv) The over reliance only on streamflow for model evaluation, which in most cases is too limited to differentiate among models, specifically calibrated models.

Wanzala et al., 2022 highlighted a procedure for preselecting models with a filter classification used for flood prediction applications in the country. The paper concentrates on six aspects of hydrological modelling; (i) Representation of the various processes (ii) Applicability of models to various climatic and physiographic backgrounds, (iii) Model resolutions and data requirements, (iv) Smaller scale downscaling capabilities (v) Accessibility of various model codes (vi) probability of operationalizing the model.

These assessments served as an objective model preselection criterion for choice of a hydrological model for use in this work.

### **2.6.2 GR4J Model**

The GR4J model, often referred to as the "Génie Rural à 4 paramètres Journalier" model, is a hydrological model utilized for rainfall-runoff modeling at the daily scale. This model was developed by researchers associated with the French National Institute for Agricultural Research

(INRA). It is a conceptual model with lumped characteristics, signifying that it represents hydrological processes at the catchment scale without explicitly considering variations in space within the catchment. It is specifically designed to simulate the conversion of rainfall into runoff and has been widely used in water resource management, flood forecasting, water resource management, and hydrological investigations.

To represent the relevant flood simulation processes within the Nzoia River Basin, and as also highlighted by (Barasa & Perera, 2018; Olang & Fürst, 2011; Onyando et al., 2003), the GR4J model was considered.

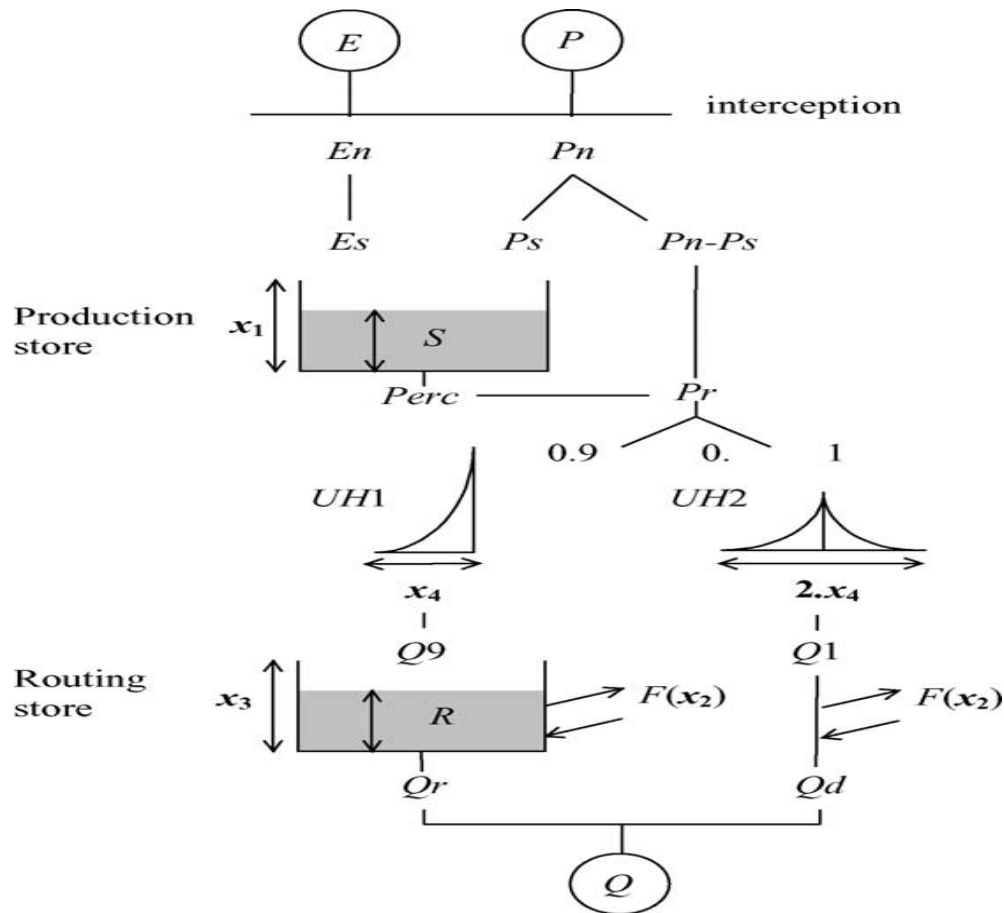


Figure 2: GR4J model diagram (Perrin et al., 2003)

The GR4J model, a lumped daily model, belongs to Soil Moisture Accounting Model (SMA) group. The model is a four parameter rainfall runoff model (Perrin et al., 2003) and an improved GR3J model version that was initially suggested by Edijatno and Michel (1989) then sequentially

upgraded by (Edijatno et al., 1999). It has been considered for this study because of its parsimonious structure, low data requirement and simplicity.

The model concept is centered on two successive reservoirs which simulate a catchment scale runoff generation development. On the first reservoir, two input parameters; Precipitation (P) and Evaporation (E) are used to simulate the soil moisture budget. The extreme production store capacity ( $X_1$ , mm), a representative threshold of the soil reservoir (S) extreme storage volume, normally controls the moisture amount retained by the soil.

The outgoing water from the first reservoir is divided in two flows: a catchment short-time response represented by a fast flow and a much slower flow, representing the slower catchment response of the system and leads to the second deposit. Part of this much slower flow leading to the second reservoir is normally defined by the groundwater exchange coefficient  $X_2$ . The threshold value of the second deposit signifies the extreme quantity of water that the system can hold is defined by the parameter  $X_3$ .

Lastly, both the slower and faster flows' routing time is determined using a unit hydrograph whose base corresponds to parameter  $X_4$ . (See figure 3). From figure 3, the unit hydrograph time base (UH1) represents the flow routing time getting into the second reservoir, while the unit hydrograph time base (UH2) represents contribution of the direct streamflow routing time and is normally twice the unit hydrograph time base (UH2).

The distinctive GR4J model inputs include potential evaporation and precipitation, both estimated within a catchment of interest. Since the model parameters are only few, simple optimization algorithms are usually able to determine the parameter values that would yield acceptable results. The consideration of the GR4J model for the study was mainly because of its uncomplicated and relatively fast calibration structure hence high performance levels (Ficchi et al., 2019).

## **2.7 Conceptual Framework**

A conceptual framework illustrating the linkage expected between the main variables – rainfall observations, potential evapotranspiration, ENSO indices and river discharge observations to be analyzed is defined in this section. The framework outlines the relevant study objectives for the

research process while mapping out how the variables come together to make comprehensible conclusions. A schematic representation of the framework for the study is depicted in Figure 1 below.

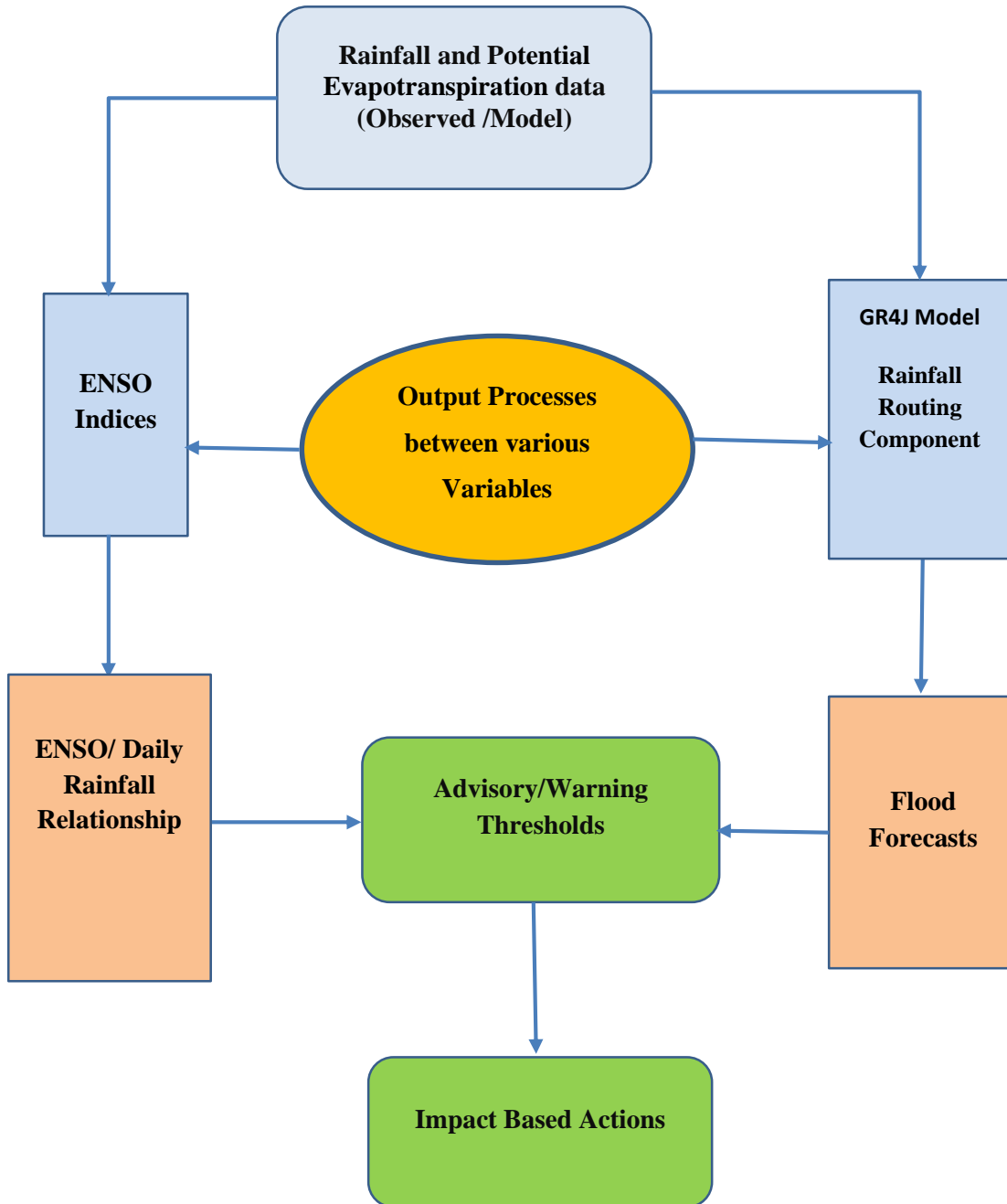


Figure 3: The conceptual framework of the study (Source: Author)



## CHAPTER THREE

### 3 DATA AND METHODOLOGY

#### 3.1 Introduction

A detailed illustration and explanation of the types and sources of data and methodology explored in the analysis to realize the study objectives is discussed in this chapter.

#### 3.2 Data

The datasets that were analyzed include daily rainfall observations from the KMD, the Climate Hazards Group Infrared Precipitation with Station data (CHIRPS), Potential Evapotranspiration (PET), Oceanic Niño Index (ONI) for ENSO analysis, and daily river discharge observations for the Nzoia River.

##### 3.2.1 Rainfall Observations

The Nzoia River Basin rainfall observations were acquired from the Kenya Meteorological Department. Four rainfall observing stations – Bungoma, Eldoret, Eldoret Airport and Kitale were used as representative stations with data from each used to analyze and assess the skill of the CHIRPS dataset considered in this study. The location coordinates of the stations used in the study are provided in Table 1 below.

*Table 1: List of stations and coordinates used in the study*

<b>LAT</b>	<b>LON</b>	<b>Nearest KMD Station</b>	<b>Mean Annual Rainfall</b>	<b>Seasonal Distribution (OND)</b>	<b>Mean Annual Variability</b>	<b>Seasonal Variability (OND)</b>
0.57	35.30	Eldoret	1266.4	250.7	18.1	38.6
0.58	34.58	Bungoma	1841.2	432.2	14.0	35.6
1.00	34.98	Kitale	1178.1	232.1	18.2	39.0
0.45	34.85	Kimilili	1260.8	243.7	18.7	39.9

### **3.2.2 Climate Hazards Group InfraRed Precipitation with Station data (CHIRPS)**

The Climate Hazards Group InfraRed Precipitation with Station datasets (CHIRPS) ranging from 1<sup>st</sup> January 1981 to 31 December 2021 were used for analysis. CHIRPS datasets, established by the United States Agency for International Development Famine Early Warning Systems Network (USAID-FEWSNET) has been used generally for analysis and monitoring of agricultural drought at different timescales including daily, decadal and monthly. The dataset consists of many years of rainfall records (from 1981 to present) and has a global coverage limit of between 50<sup>0</sup>S–50<sup>0</sup>N latitude.

It is a gridded rainfall dataset created by a combination of a 0.05<sup>0</sup> by 0.05<sup>0</sup> spatial resolution infrared satellite data and station observations. (Funk et al. 2015 ). The dataset has been considered for the study due to its large coverage, fairly high resolution, low bias and the availability of records available over long periods.

Over East Africa where there is a robust association between rainfall and ENSO variability, CHIRPS datasets have been vital for enhanced drought and famine emergency anticipation, hence making available important information for humanitarian organizations working responses to extreme climatic conditions. (Wenhaji Ndomeni et al., 2018).

The need for a combination of a long duration of rainfall dataset and high skill in prediction and application led to the consideration of the CHIRPS for this study.

### **3.2.3 Potential Evapotranspiration (PET)**

The Potential Evapotranspiration (PET) data is a resultant dataset of the FAO's Penman-Monteith formulated using ERA5-Land climate variables (Bliss et al., 2021). The PET dataset used in the study covered the time period between 1981 to 2021 and was at 0.1 degrees' global land area spatial resolution.

### **3.2.4 ENSO Indices**

Sea surface temperature, an important climate variable is an essential indicator of the global climate. SST datasets have been widely used in the monitoring and simulation of climate with several datasets developed by global centres and updated on a monthly timescale. For this study, the Oceanic Niño Index (ONI) was considered to define the El Niño-Southern Oscillation. ONI, a primary index for classifying and monitoring the ENSO strength as defined by NOAA. It uses a 3-month rolling SST averages within the East and Central Tropical Pacific region commonly called the Niño 3.4 region. ONI values of +1.0 and higher were considered to define strong El Niño years in the study. (Kousky & Higgins, 2007).

### **3.2.5 Daily River discharge observations**

To determine the linkage between flooding and extreme rainfall within the Nzoia River Basin, daily discharge observations spanning from 1<sup>st</sup> January 1981 to 31<sup>st</sup> December 2021 at River Gauging station 1EE01 were utilized. The River Gauging station 1EE01 was considered because of its location on the Lower Nzoia Basin which normally experiences most flooding over the basin.

## **3.3 Methodology**

### **3.3.1 Time Series Analysis**

To determine the performance of the CHIRPS dataset before being used for further analysis, time series plots analysis were carried out for CHIRPS data against the four representative station observations. The CHIRPS dataset analyzed was gotten by extracting a grid box over each of the representative stations within Nzoia Basin. Further, Pearson correlation coefficient analysis was carried out to determine the level and strength of relationship between the two datasets.

To determine the temporal variation of monthly rainfall data, time series plots were again considered to evaluate the temporal evolutions of the data. For this study, the mean monthly rainfall totals for the four stations were plotted for the CHIRPS dataset used in the study to assess the annual variability

### **3.3.2 Spatial-temporal Analysis**

To determine a comprehensive picture of rainfall across the Nzoia Basin, the rainfall data obtained was subjected to spatio-temporal analysis. Analysis entailed an identification of trends or patterns

in the rainfall data, such as deviations in the intensity and frequencies of rainfall events over the years. The mean annual rainfall was determined by summing the long term averages for the twelve months.

The coefficient of variation, a measurement of variation which compares the standard deviation to the mean which mainly provides an indication of the dependability of rainfall patterns. The coefficient of variation depicting the dependability of the rainfall within a given area was derived by dividing the standard deviation by the rainfall averages and expressed as a percentage.

$$CV = \frac{SD}{Mean} \times 100 \quad \text{Equation 1}$$

Whereby;

CV = Coefficient of Variation

SD = Standard deviation

A higher variability typically implies a lower dependability of the rainfall while a lower variability the reverse. For monthly rainfall values, cases below 100% of Coefficient of variation were considered dependable, while those more than 100% not dependable rainfall. For this study, the coefficient of variability was calculated for long term mean annual rainfall.

On the precipitation ratio was used to determine the anomalies of rainfall within a specific region. The precipitation ratio was considered to give an indication of rainfall stability with a spatial pattern. The higher the ratio, the higher the rainfall anomaly while lower ratios depicts a lesser anomaly. The precipitation ratio was determined using the formula below;

$$PR = \frac{P_x - P_n}{P_m} \times 100 \quad \text{Equation 2}$$

where;

PR = Precipitation Ratio

P<sub>x</sub> = Maximum of Rainfall

P<sub>n</sub> = Minimum of Rainfall

$P_m$  = Mean Rainfall

The spatial analysis of rainfall data for the basin was performed using geospatial techniques. Data points for representative stations were first extracted and processed before various indices - rainfall totals, coefficient of variation and precipitation ratio computed. Afterwards, grid points were converted to shape file formats in the Universal Transverse Mercator (UTM) projection before generating interpolations using the IDW technique.

### **3.3.3 Box and whisker plots**

For ENSO effects on the daily rainfall patterns over the Nzoia Basin, CHIRPS data between the period of 1981 to 2021 was examined. The methodology entailed the identification of strong El Nino years defined by ONI values greater than +1 in the rainfall data period.

However, it is imperative to highlight that both El Nino or La Nina events normally starts to develop averagely around August/September and reach their maximum around December/January before decaying through until around April/May. This therefore means that the maximum ONI values considered for the study were observed during the OND season.

For this study, this whole period is defined as an ‘El Nino event’. For this reason, to look at a whole period of an El Nino event, normal years were shifted from a calendar year of January – December to August - July as my year so that it covers the whole el Nino event period. For instance, for an El Nino that started in September 2009 and finished in May 2010, daily rainfall data between August 2009 and July 2010 were analyzed.

The relationship between ENSO and daily rainfall within the Nzoia River Basin was determined through statistical analysis using the box and whisker plots. Box and whisker plots would represent the distributions of historical daily rainfall linked to the three ENSO phases over Western Kenya. Box and whisker plots are considered as it normally outlines important summaries various characteristics datasets like central tendencies, extreme and dispersions. The above characteristics are normally arrived at through analysis of percentile ranks and minimum and maximum values in a box and whisker plot.

The technique has also been considered for this study as its provides the best way to identify asymmetrical attributes in a dataset. Furthermore, the fundamental statistics are more resilient

toward distinct outliers compared to other methods like the standard deviation and the mean. Also, box and whisker plots' graphically compact nature enables side-by-side assessment of several data, data extremes and results from different stations, which can normally be challenging to understand or interpret by way or means of other representations like the histogram.

### **3.3.4 Significance Tests**

Significance tests were performed on the results obtained from the ENSO/daily rainfall relationship. For the rainfall distributions during the El Nino years analyzed, statistical significance testing of the results was considered, to test whether the variations in the rainfall distribution was due to chance or ENSO influence. The Monte Carlo resampling method of testing statistical significance of a distribution was considered.

#### **3.3.4.1 Monte Carlo Simulation/Resampling**

Monte Carlo simulation is a technique of statistical simulation which computes results based on statistical analysis of recurring random sampling. The simulation method is very closely linked to random experimentations, for which the explicit results are not known beforehand. For this study, Monte Carlo technique was preferred for testing the statistical significance of the results, to test whether the variations in the rainfall distribution were due to chance because of the limited sample size of data.

For a given strong El Nino year, the median for all of the rainfall data was determined for all the days with rainfall greater than 1mm. Randomly selected days equivalent to the rainfall days greater than 1mm for a given strong El Nino year were selected from the whole dataset (whole data). The median for this random sample was then determined with the process being repeated 1000 times, with the medians being saved each time that so that there were 1000 medians. The original median for each strong El Nino year was then compared against these 1000 values.

A characteristic feature of the Monte Carlo resampling method is that the distinctive values (medians, quantiles, means to definite values of  $y$ , etc.), gotten as an outcome of  $n$  trials, are not always the same in any two sets of simulations. The results are therefore only an estimate, but they are closer to the actual values for more trials. For this case, if the median is outside the range of 90% of the 1000 medians (i.e., if the median of the original distribution is less than the 5th

percentile, or greater than the 95th percentile), then the result was considered statistically significant at the 90% confidence level.

### **3.3.5 GR4J Model Calibration/Validation**

The calibration and validation of the GR4J model was done by dividing the data into sub periods indicated in Table 5. These sub periods were selected based on an analysis of the stationary breaking in the rainfall and discharge time series, ensuring that the sub periods were homogenous. To calibrate the model, 65% of the entire dataset was utilized. The calibration period spanned from 1<sup>st</sup> January 1982 to 31<sup>st</sup> December 2000 with the year 1981 being used for model warm-up period specifically for calibration purposes. During this period, the model was prepared for the calibration process, but the results were not considered in the final calibration score computation. Following the calibration phase, the model was then validated using the remaining 35% of the data. The validation period extended from 1<sup>st</sup> January 2002 to 31<sup>st</sup> March 2018. Similarly, the year 2001 was set as the validation warm-up period for the validation process. This validation warm-up period allowed the model to adjust to the new data and ensured that the results obtained during this time were not included in the final validation analysis. The aim of dividing the data into these distinct sub periods was to evaluate the performance and accuracy of the GR4J model in simulating rainfall and discharge. Both the calibration and validation processes allowed for the evaluation and refinement of the model's parameters and performance ensuring its reliability in predicting hydrological phenomena.

To optimize the model parameters and for measurement of model performance for flow simulations, the Nash-Sutcliffe efficiency (NSE) criterion that is centered on the goodness-of-fit approach was considered for evaluation (Nash & Sutcliffe, 1970). According to evaluation Nash & Sutcliffe, 1970, the NSE criterion is calculated based on four options – flow square roots, high water flows, flow logarithms and a criterion based on the balance sheet. The range of parameters used to calibrate the model and for initial runs are those also presented in Perrin et al., 2003. For these four options, it is the criterion based on flow of high water which was considered for this study. This criteria of flows of high water can be expressed by the formula below;

$$NSE = 1 - \frac{\sum_{i=1}^n (Q_{sim} - Q_{obs})^2}{\sum_{i=1}^n (Q_{obs} - Q_{mean})^2} \quad \text{Equation 3}$$

Where;

$Q_{sim}$  = Simulated daily runoff

$Q_{obs}$  = Observed daily runoff

$Q_{mean}$  = Mean daily runoff



## CHAPTER FOUR

### 4 RESULTS AND DISCUSSIONS

#### 4.1 Validation of CHIRPS

The time series plots indicating the performance of the CHIRPS data against the four representation station observations are depicted in Figure 4 (a-d) below. The CHIRPS dataset analyzed was gotten by extracting a grid box over each of the representative stations within Nzoia Basin.

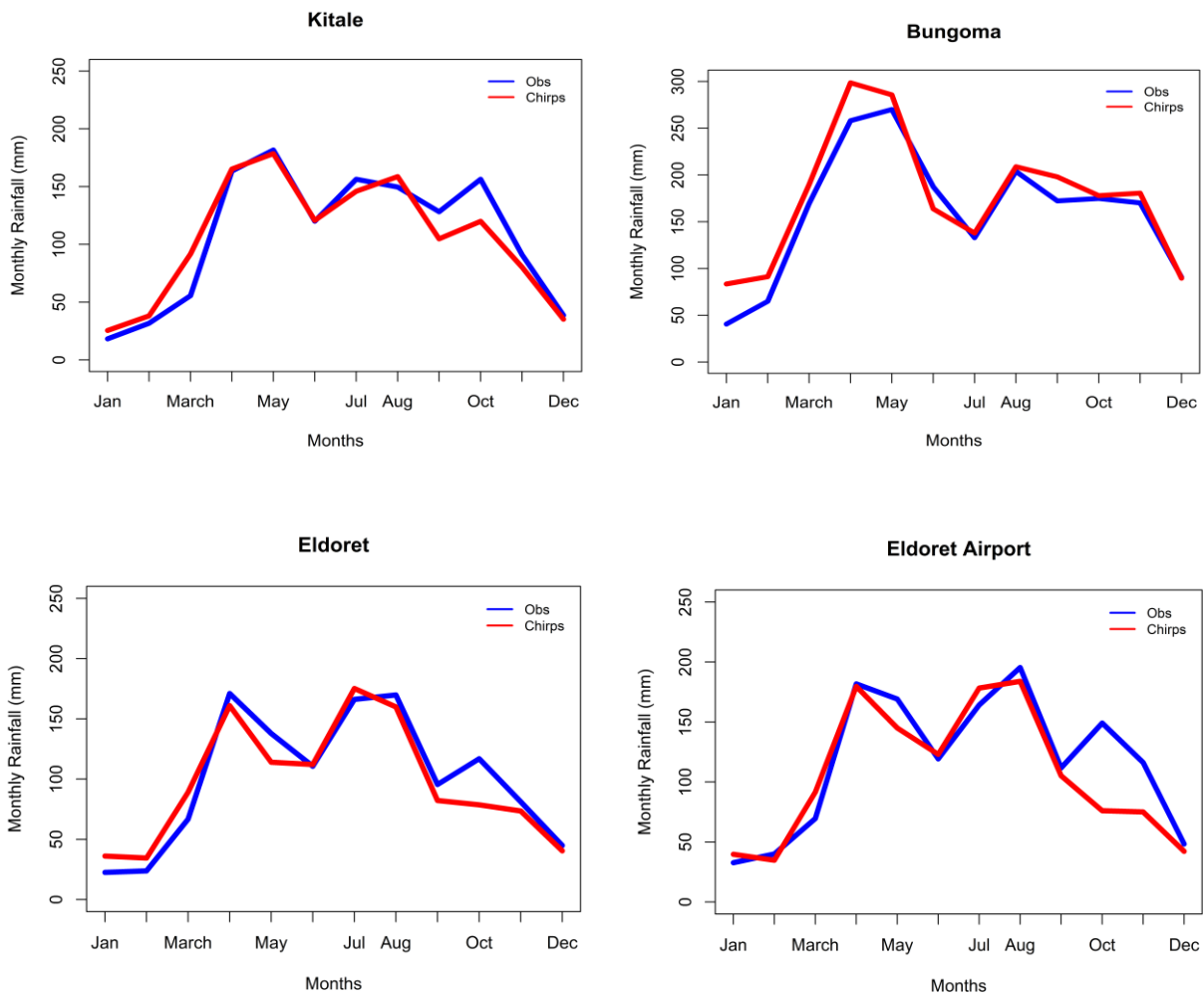


Figure 4: Comparison between CHIRPS and station(observed) rainfall data . The x-axis represents the time period in months

Figure 3 clearly indicates data consistency between CHIRPS data and observed data. The close match in the time series depicted by the plot indicates an agreement between the observed rainfall observations and the CHIRPS datasets.

*Table 2: Table of Pearson correlation (r) between observed and Chirps data*

<b>Station</b>	<b>Pearson correlation (r)</b>
Kitale	0.95
Eldoret	0.95
Bungoma	0.96
Eldoret Airport	0.89

From Table 1, there is a high Pearson correlation coefficient of above 80% (0.80) between the station observations and the CHIRPS data for the mentioned stations implying a strong similarity in the precipitation patterns captured by CHIRPS.

Other studies which have also used CHIRPS dataset as a proxy for observed data for Kenya and East Africa include (King et al., 2021; Le & Pricope, 2017a; Omay et al., 2023 and Wanzala, Stephens, et al., 2022 ). This indicates that CHIRPS data can be a reliable and accurate source for assessing precipitation in these locations.

## **4.2 Objective 1 - Spatial and Temporal Rainfall Distribution**

The objective one results, comprising the analysis of spatio-temporal variations of rainfall within the basin is presented in this section.

### **4.2.1 Spatial Distribution**

For spatial rainfall distribution, the collected rainfall data was analyzed using three rainfall indices to define the spatial distribution within the basin. The precipitation ratio, mean seasonal (OND) and annual rainfall totals and coefficient of rainfall variation are considered to define the basin rainfall characteristics. The final analysis results were mapped using GIS to get spatial outlooks. Table 2 depicts a summary of the rainfall indices analyzed with a few data points within the study area.

*Table 3: Annual and Seasonal Rainfall Distribution summary for Nzoia River Basin*

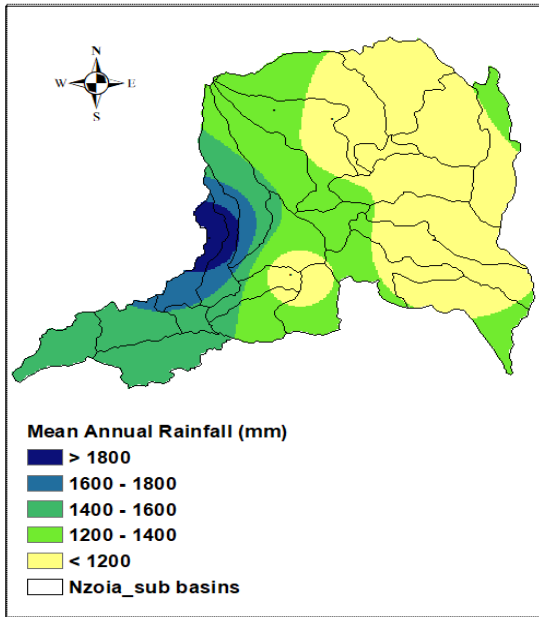
<b>LAT</b>	<b>LON</b>	<b>Nearest KMD Station</b>	<b>Mean Annual Rainfall</b>	<b>Seasonal Distribution (OND)</b>	<b>Mean Annual Variability</b>	<b>Seasonal Variability (OND)</b>
0.57	35.30	Eldoret	1266.4	250.7	18.1	38.6
0.58	34.58	Bungoma	1841.2	432.2	14.0	35.6
1.00	34.98	Kitale	1178.1	232.1	18.2	39.0
0.45	34.85	Kimilili	1260.8	243.7	18.7	39.9

*Table 4: Annual and Seasonal Rainfall Precipitation Ratios for Nzoia Basin*

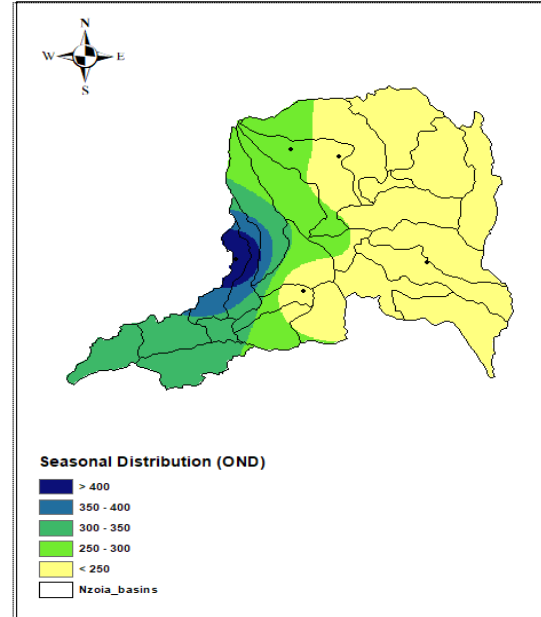
<b>LAT</b>	<b>LON</b>	<b>Nearest KMD Station</b>	<b>Annual Precipitation Ratio</b>	<b>OND Precipitation Ratio</b>
0.57	35.30	SCC, Eldoret	101.1	152.5
0.58	34.58	Bungoma	77.5	149.3
1.00	34.98	Kitale	103.0	151.1
0.45	34.85	Kimilili	103.6	155.3

#### **4.2.1.1 Annual and Seasonal Rainfall Distribution**

For the study area, the mean annual averages ranged between slightly below 1200mm and above 1800mm. From Figure 5 below, it is evident that the western region of the basin receives more annual rainfall, averaging above 1400mm compared to the Eastern part at around 1200mm. Figure 5 (a) shows the spatial distribution of the mean annual rainfall over the basin.



(a)



(b)

*Figure 5: (a) Mean Annual Rainfall and (b) Seasonal (OND Season) Rainfall Distribution*

For OND seasonal rainfall distribution (Figure 5(b)), a similar spatial distribution pattern to the annual rainfall distribution is evident. However, it's worth noting that the OND season contributes a smaller rainfall amount to the annual share with a seasonal total variation of around 250mm to slightly above 400mm. The OND rainfall maximum rainfall also occurs in the western parts of the basin around the Mt. Elgon. It is also evident from the spatial maps that the seasonal distribution is more concentrated on the western regions of the study area with the eastern sides having lesser values. On the other hand, the mean annual distribution depicts pockets of higher values also on the eastern part of the basin.

#### 4.2.1.2 Mean Annual and Seasonal Rainfall variability

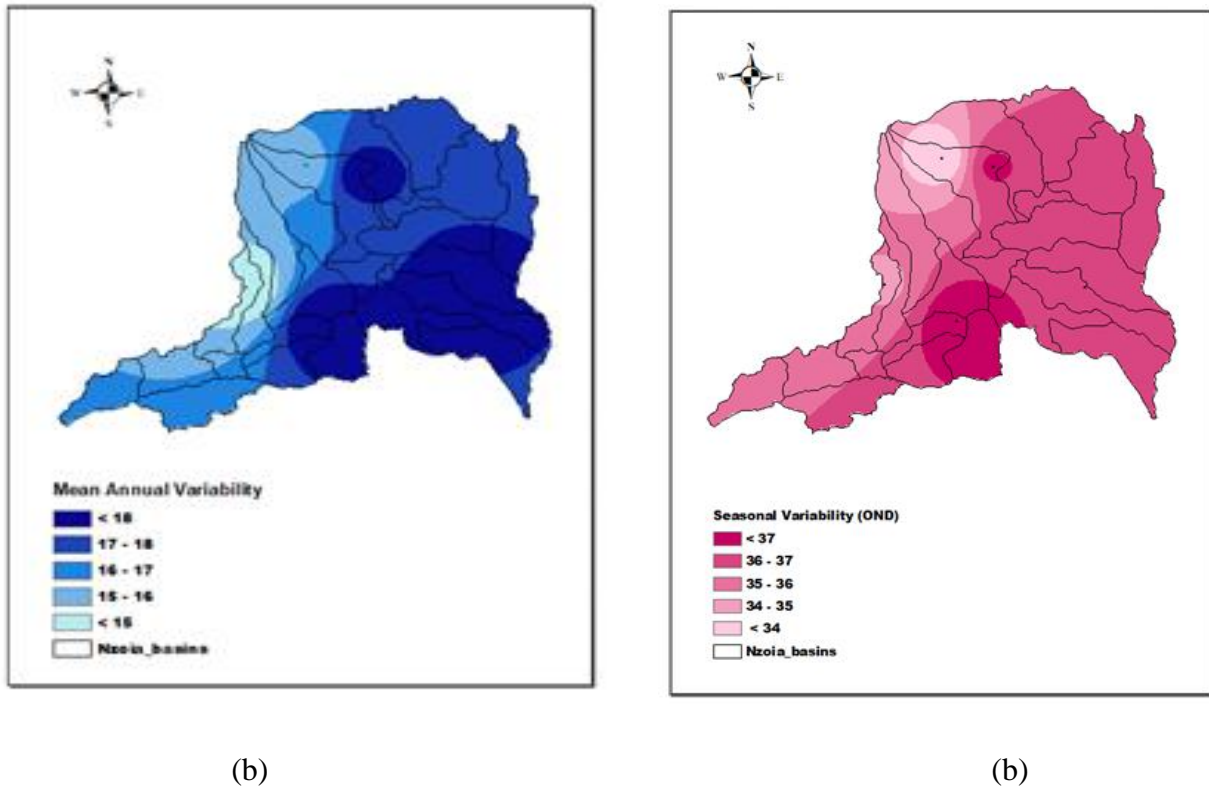


Figure 6: (a) Mean Annual Precipitation Ratio and (b) Seasonal (OND) Precipitation Ratio

From the results obtained, the coefficient of variability of the basin is seen to range between 15% to 18% (Figure 6a). Minimum variability is found mostly within the western parts of the basin area with a variability of around 15% to 16% indicating a higher level of dependability in terms of rainfall patterns with the reverse evident around the eastern parts at 17% to 18% indicating a relatively less dependable rainfall pattern distribution.

For OND season rainfall variability, the Figure 6b provides an insight of the basin variability. Slightly higher variations are found compared to the annual values. A range of variability of between 35% to 37% concentrates around the eastern parts of the basin area suggesting a less dependable rainfall during this season in this region. However, lower variability range of around 34% to 35% is seen more on the western parts mostly around the Mt. Elgon area indicating a relatively more dependable rainfall distribution during the OND season in these areas. The high OND rainfall variability compared to the annual variability suggest a less occurrence of rainfall

during OND compared to the annual distribution. This is true as earlier found under the analysis of the mean annual and seasonal rainfall distribution.

#### 4.2.1.3 Annual and Seasonal Precipitation ratio

Figure 7(a), clearly shows that the mean annual precipitation ratio exhibits a lower value in the western region, gradually increasing towards the eastern part. Specifically, in the western section, the ratio ranges from 85mm to 90mm, while in the eastern part, it surpasses 95mm. This implies a trend of an increase in precipitation from the western to eastern parts of the basin.

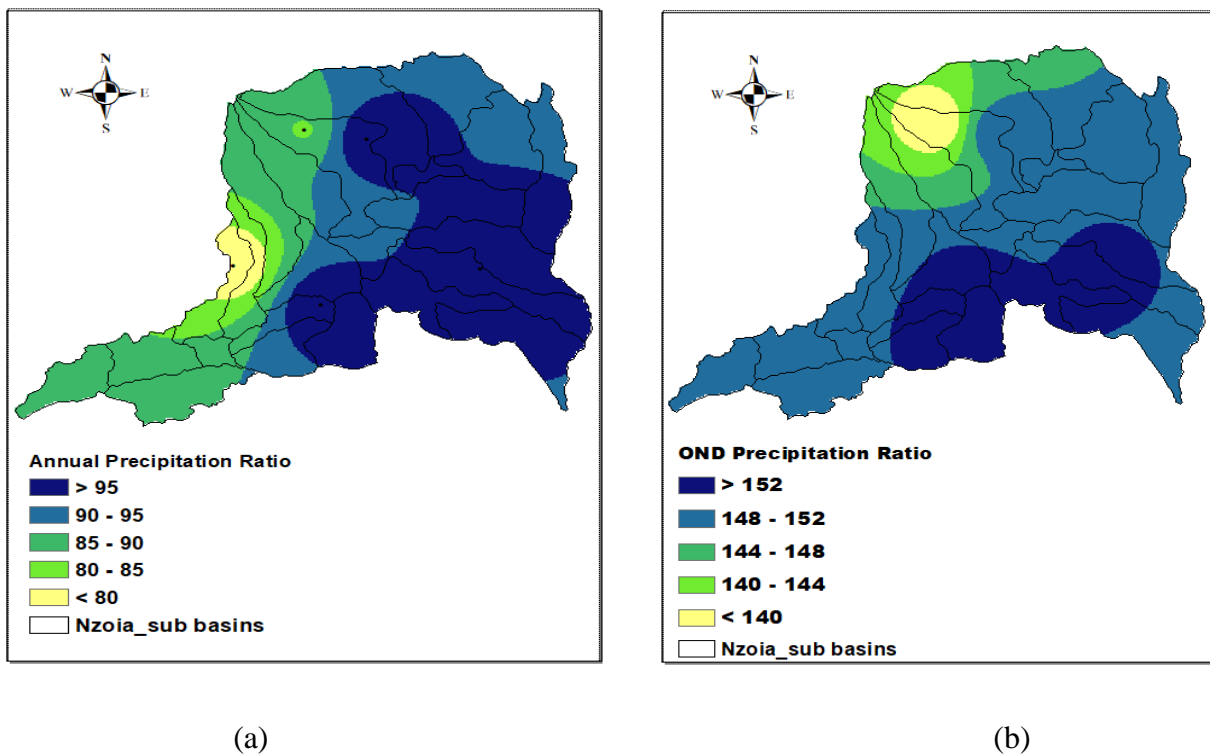


Figure 7: Mean Annual Precipitation Ratio (a) and OND (Seasonal) Precipitation Ratio

For comparisons between seasonal and annual precipitation ratios, Figure 7 indicates that the western part has higher OND ratios compared to the mean annual precipitation ratio. Over the western region, the ratio ranges from 148mm to 152mm with an increase towards the east, surpassing 152mm. However, in the furthest east, the ratio reduces and falls within the range of 148mm to 152mm. In terms of spatial variability, the precipitation ratio demonstrates overall high

values across the sub basin. This indicates that the distribution of rainfall was not uniform throughout the Nzoia sub basin, as certain locations received significantly higher amounts of rainfall compared to others.

There is an increasing trend of precipitation from the western to the eastern part as evident from the mean annual precipitation ratio. The OND precipitation ratio indicates higher values in the western region compared to the annual ratio.

#### 4.2.2 Temporal Distribution of Daily Rainfall

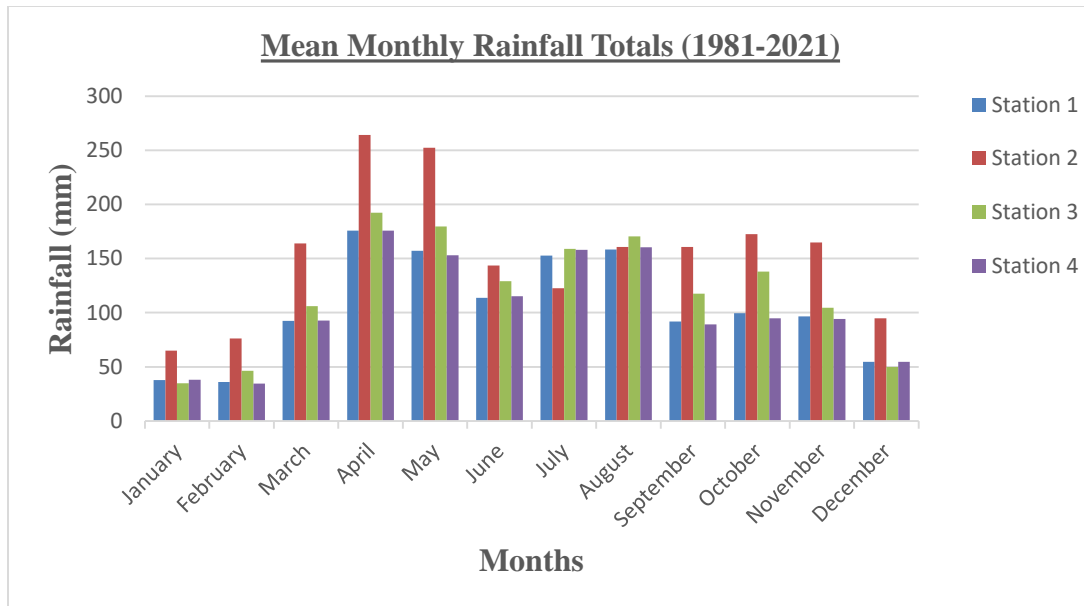


Figure 8: Monthly Rainfall Distribution with the Nzoia Basin

Figure 8 clearly indicates that Station 2 consistently recorded the highest mean monthly rainfall in most years, apart from for the months of July and August when Station 3 had the highest values. In general, the peak rainfall across all four stations occurred during the March to May season, which represents the long rainy season in Kenya. Specifically, the highest mean rainfall of 264mm was recorded in April, while the lowest mean rainfall of 34mm occurred in February. The data indicates that Station 2 consistently received the highest average rainfall throughout the year, with exceptions in July and August when Station 3 surpassed it. However, during the MAM season, all stations registered their highest rainfall values indicating the peak period for rainfall in the region.

The specific month of April had the highest mean rainfall of 264mm, suggesting it is a critical period for precipitation in the basin area. On the other hand, February recorded the least mean rainfall of 34mm, highlighting it as a relatively drier period compared to other months.

### 4.2.3 Spatial Distribution of Potential evapotranspiration

From Figure 9(a) and (b) which are the Mean Annual Potential Evapotranspiration (PET) and Seasonal (OND) distribution, the analysis of the spatial distribution of potential evapotranspiration nearly similar in both cases.

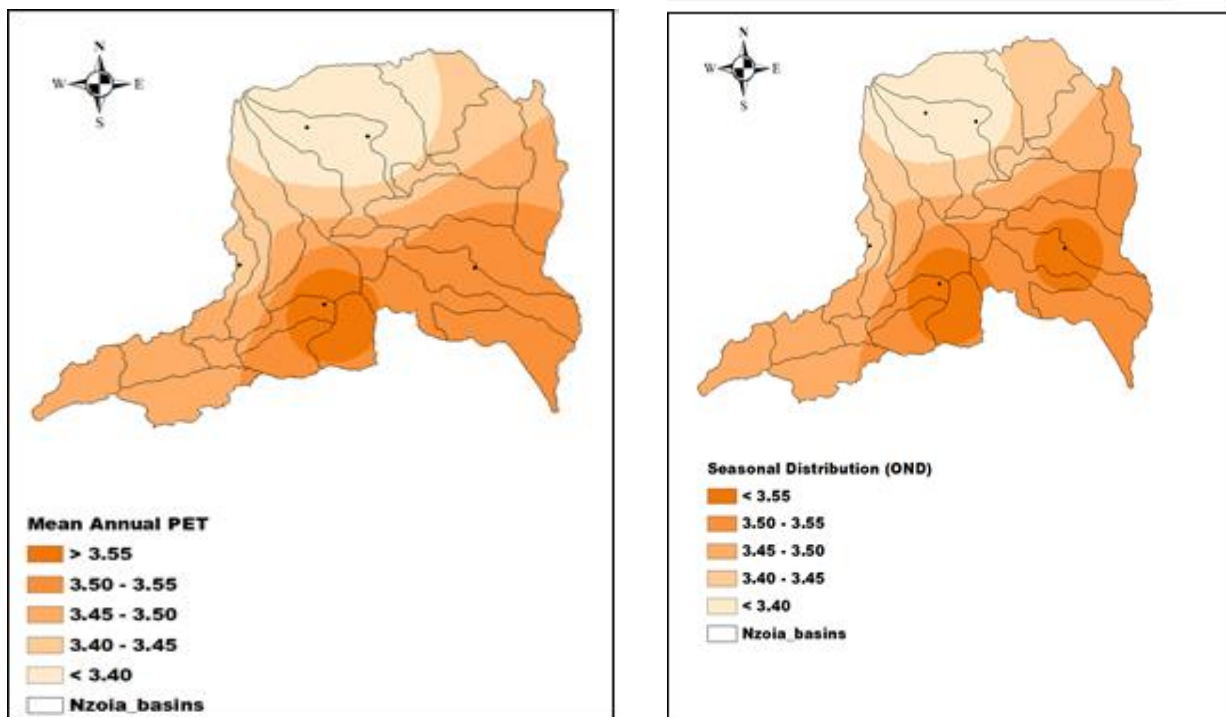


Figure 9: Mean Annual Potential Evapotranspiration (a) and Seasonal (OND) Distribution (b)

In both figures, the western region displays a range of mean annual PET values between 3.40mm and 3.45mm, which progressively increases towards the eastern side, reaching a range of 3.50mm to 3.55mm. Moreover, the central region exhibits relatively higher values with a mean annual PET of 3.55mm and above. The figures also demonstrate a consistent spatial pattern of PET across the Nzoia basins. The western side consistently experiences lower PET values, indicating relatively lower potential evapotranspiration rates. Conversely, as we move towards the eastern side, PET values gradually increase, suggesting higher rates of potential evapotranspiration. The central



region stands out with the highest PET values, signifying a zone characterized by enhanced evapotranspiration processes.

#### 4.2.4 Temporal Variation of Potential evapotranspiration

The mean annual cycle for the potential evapotranspiration (PET) data was analyzed for the period 1981 to 2021. The mean annual cycle for PET in this study was defined as the monthly average of the available hourly observations between the period 1981 to 2021.

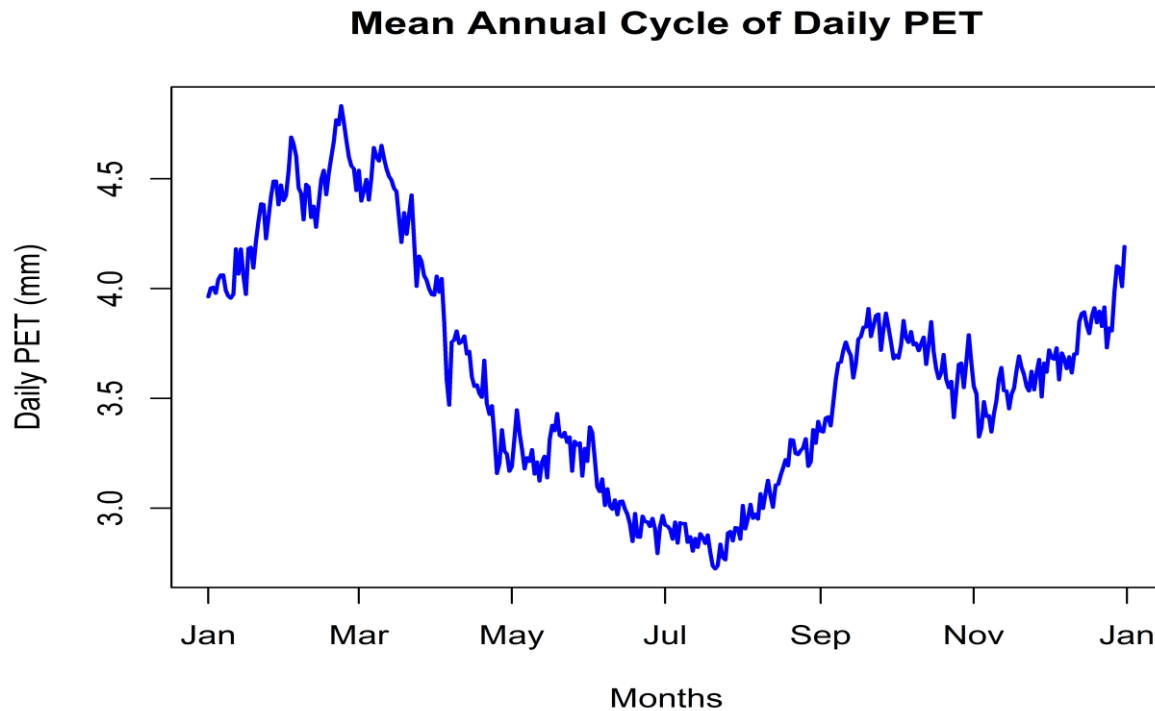


*Figure 10: Temporal Variation of the Spatial Average of the Potential Evapotranspiration in Nzoia Basin*

From the results depicted in Figure 10, the mean PET exhibits distinct temporal variation with a sharp decrease from May to August before increasing comparatively quickly towards the end of the year. The time series shows that the highest PET values were observed during the month of March with August recording the lowest PET values. March is the period with the highest average potential evapotranspiration, indicating a significant demand for water due to atmospheric conditions and environmental factors during that time. On the other hand, August experiences the

lowest mean PET values suggesting relatively cooler and less demanding conditions for water loss through evapotranspiration.

### 4.3 Objective 2 - ENSO effect on Rainfall Distribution

For the second objective, the ENSO response to daily rainfall patterns was examined over the study area using the CHIRPS data for the period 1981 to 2021. The ENSO index, Oceanic Niño Index (ONI) was first used to categorize strong El Niño years to be considered for further analysis. Strong El Niño years for this study was defined as years with ONI index greater than +1.0. A time series plot of ONI values between 1980 and 2021 is shown in Figure 11. This result reveals the extreme wet and dry years as indicated by red and blue lines respectively.

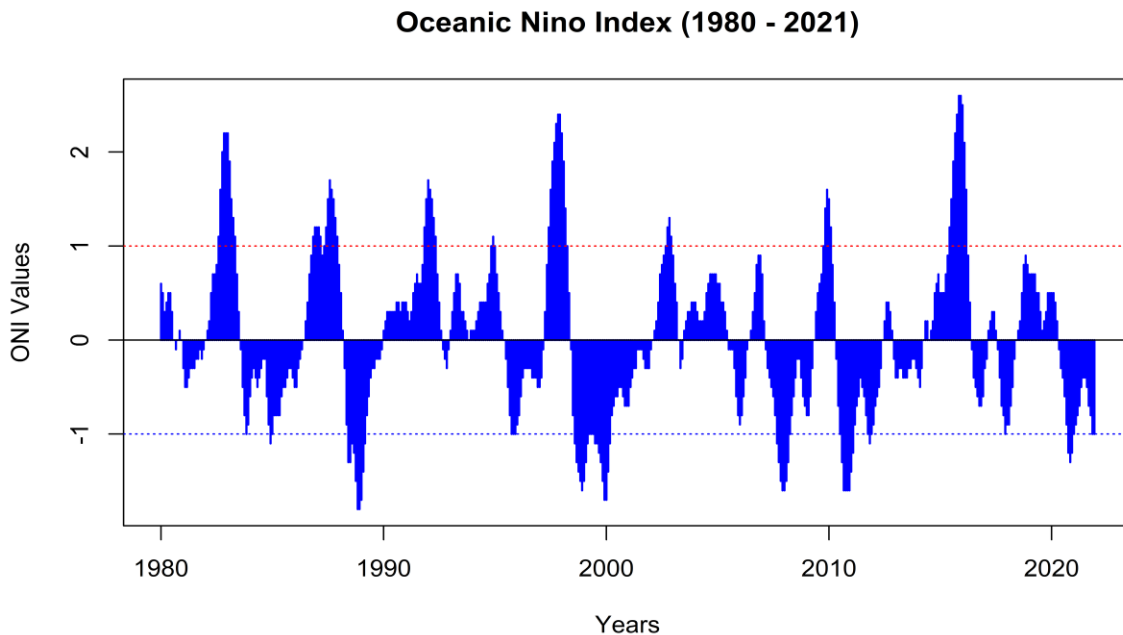


*Figure 11: Mean Annual Potential Evapotranspiration (a) and Seasonal (OND) Distribution (b). The Red and Blue dashed lines represent thresholds for strong El Niño and La Niña respectively*

Further, after analyzing the ONI indices, the extremely wet (El Niño) years considered for further analysis in this study are summarized in Table 4 below.

Table 5: El Nino Years Considered for the study

El Nino Years	Maximum ONI Values
1982/1983	2.2
1986/1987	1.2
1987/1988	1.6
1991/1992	1.7
1994/1995	1.1
1997/1998	2.4
2002/2003	1.2
2009/2010	1.6
2015/2016	2.6

The probability of daily response to ENSO was first determined and compared to the rainfall probability of the entire dataset. For each rainfall station (data point) being analyzed, daily rainfall greater than 1mm and extreme values (95<sup>th</sup> percentiles) were considered (Figure 11 and 12).

#### 4.3.1 Rainfall distribution greater than 1mm

To determine the influence of ENSO on the distribution of rainfall within the basin, a box-and-whisker plot of all rain days together with separate box-and-whisker plots for each strong El Nino years (ONI>1) were plotted to see a shift in the rainfall distribution during El Nino years. To determine how ENSO, change the probability of rainfall, an initial minimum threshold value of 1mm was considered using all the days, then the probability of rainfall using only strong El Nino years. (Figure 12)

To determine the impact of ENSO on the spatial distribution of rainfall within a specific basin, a box-and-whisker plot was generated to visualize the distribution of rainfall on all the rainfall days within the basin. Another separate box-and-whisker plots were created specifically for the years characterized by strong El Niño years (indicated by ONI values greater +1.0). The box-and-whisker plot for all the rainfall days provided a comprehensive overview of the rainfall distribution within the basin, showcasing the spread of rainfall amounts, the median rainfall value, and any

potential outliers. By examining this plot, any significant shifts or variations in the rainfall distribution during El Niño years could be identified. To further investigate how ENSO influences the probability of rainfall, an initial threshold of a minimum amount of 1mm of rainfall was established. This threshold was applied to all days within the dataset, regardless of ENSO conditions. Subsequently, the probability of rainfall exceeding this minimum threshold was calculated using data exclusively from the strong El Niño years. Strong El Niño years were defined based on the ONI, which is a measure of the deviation in sea surface temperatures in the tropical Pacific Ocean. Strong El Niño years were characterized by ONI values exceeding 1, indicating a substantial departure from average sea surface temperatures and a pronounced El Niño event. The reason for quantitatively evaluating the probability of rainfall exceeding the 1mm threshold during strong El Niño years was to ascertain any notable changes in the likelihood of rainfall occurrence compared to the overall rainfall distribution across all years. (Figure 12) presents the resulting plots, allowing for a visual comparison of the rainfall distribution on all rainfall days with the distribution during strong El Niño years.

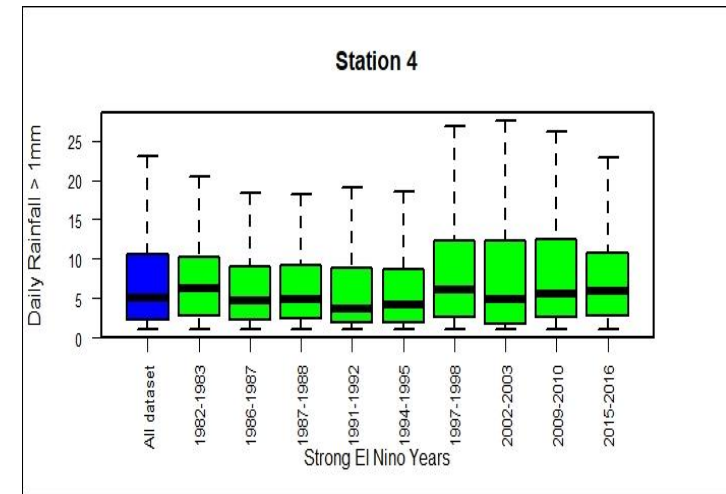
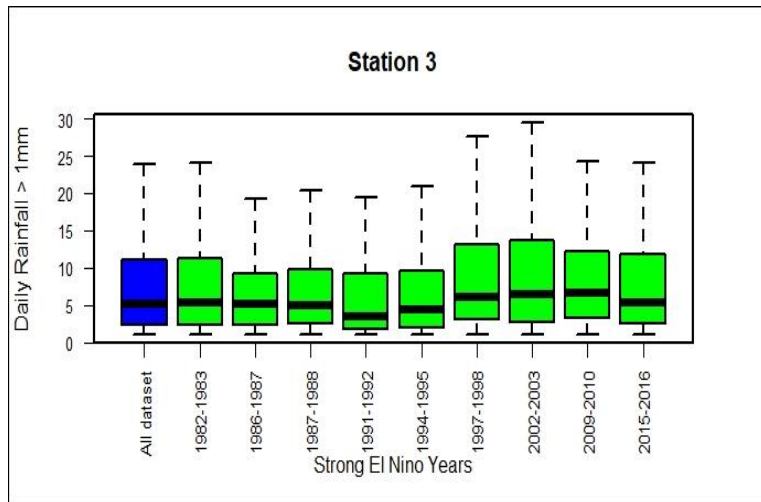
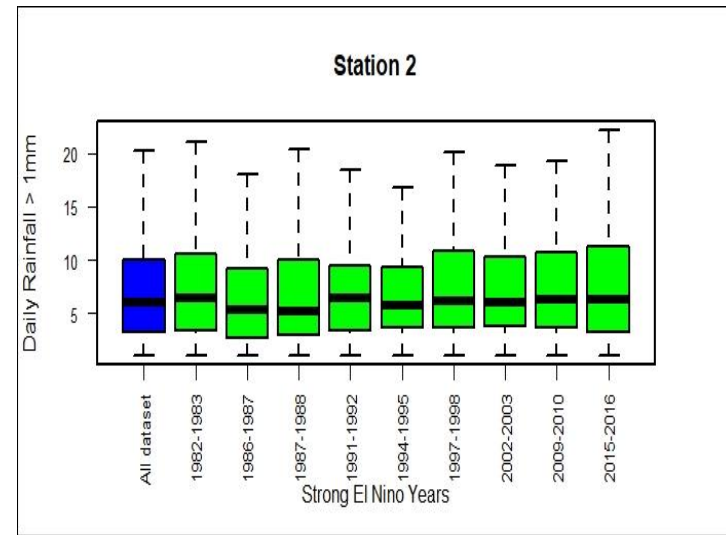
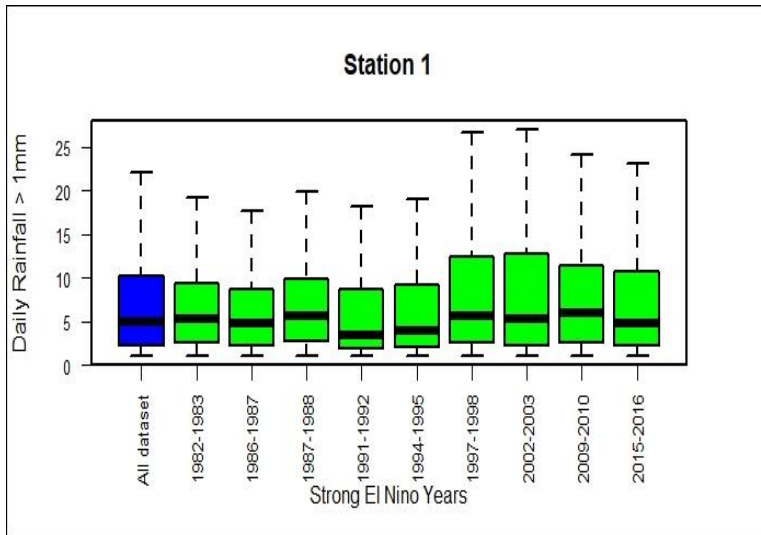


Figure 12: Box and whisker plots of daily rainfall greater than 1mm for the whole dataset (blue box) and strong El Niño years (green boxes)

### 4.3.2 Extreme daily rainfall distribution (95<sup>th</sup> Percentile)

For the extreme rainfall distribution, a similar analysis to the previous one was conducted. However, this time, the focus shifted to extreme rainfall occurrences. In order to identify extreme rainfall events, a different threshold was employed. Instead of using a fixed minimum amount of rainfall, a relative threshold was applied, specifically the 95<sup>th</sup> percentile of rain rates observed at each station within the basin. The 95<sup>th</sup> percentile was determined using the equation below;

$$R = \frac{95}{100} \times n \quad \text{Equation 4}$$

where;

R = Rank/ 95<sup>th</sup> Percentile

n = number of data points for the individual ENSO year

This ensured that extreme values were captured in a station-specific manner. The analysis was then carried out separately for each strong El Niño year, where strong El Niño events were defined based on an ONI value exceeding 1. The aim of examining the extreme rainfall distribution during these specific years was to investigate the impact of strong El Niño events on extreme daily rainfall. The results depicted in (Figure 13), revealed a higher variability in the response of extreme daily rainfall (95<sup>th</sup> percentile) to strong El Niño events compared to the analysis considering rainfall greater than 1mm as shown in (Figure 12). This suggests that the influence of El Niño on extreme rainfall events is more pronounced and varied. However, the overall distribution of extreme rainfall during El Niño years did not exhibit substantial differences compared to the non-El Niño years. Some El Niño events had a lesser impact on extreme rainfall despite their high magnitudes. This observation was particularly evident in the case of the 2015/2016 event, which had the greatest magnitude among the analyzed El Niño events but exhibited a lesser impact on extreme rainfall compared to previous, less intense El Niño events.

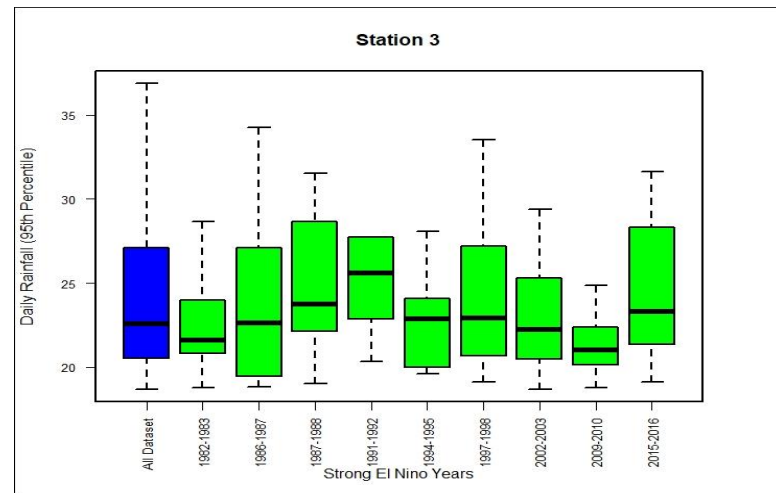
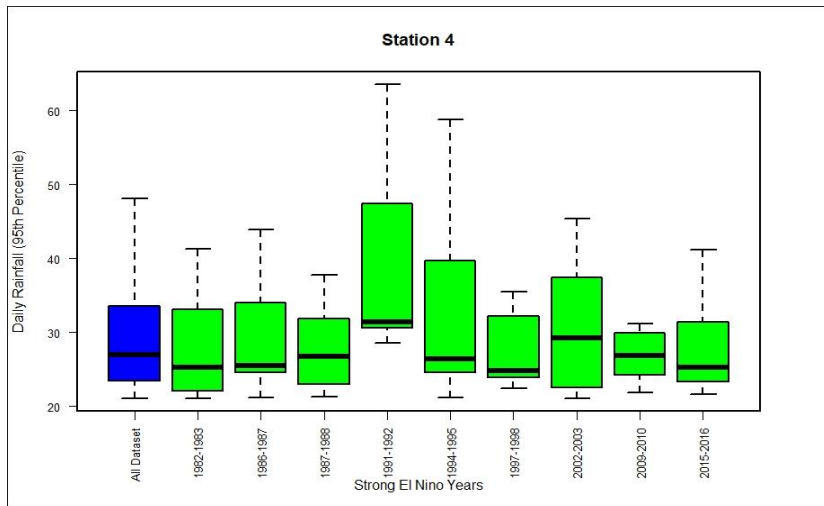
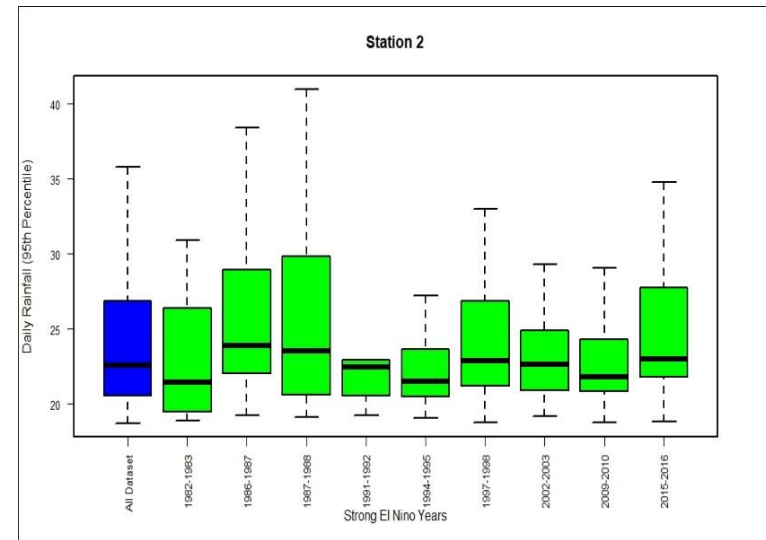
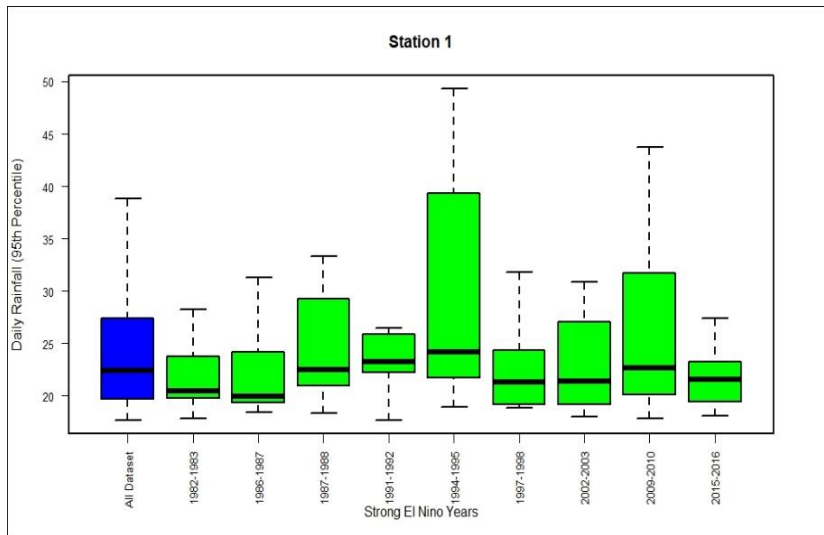


Figure 13: Box and whisker plots of daily rainfall above 95<sup>th</sup> Percentile the whole dataset (blue box) and strong El Niño years (green boxes)

From the results depicted in Figure 14 and 15, it is evident that the median for all the strong El Nino years analyzed were either smaller or greater than the 90% of the 1000 medians (Monte Carlo Medians) i.e., the median of the original distribution was either less than the 5th percentile, or greater than the 95th percentile. This therefore means that the analysis obtained from the extreme daily rainfall (greater than 95<sup>th</sup> Percentile) were statistically significant at 90% confidence level.



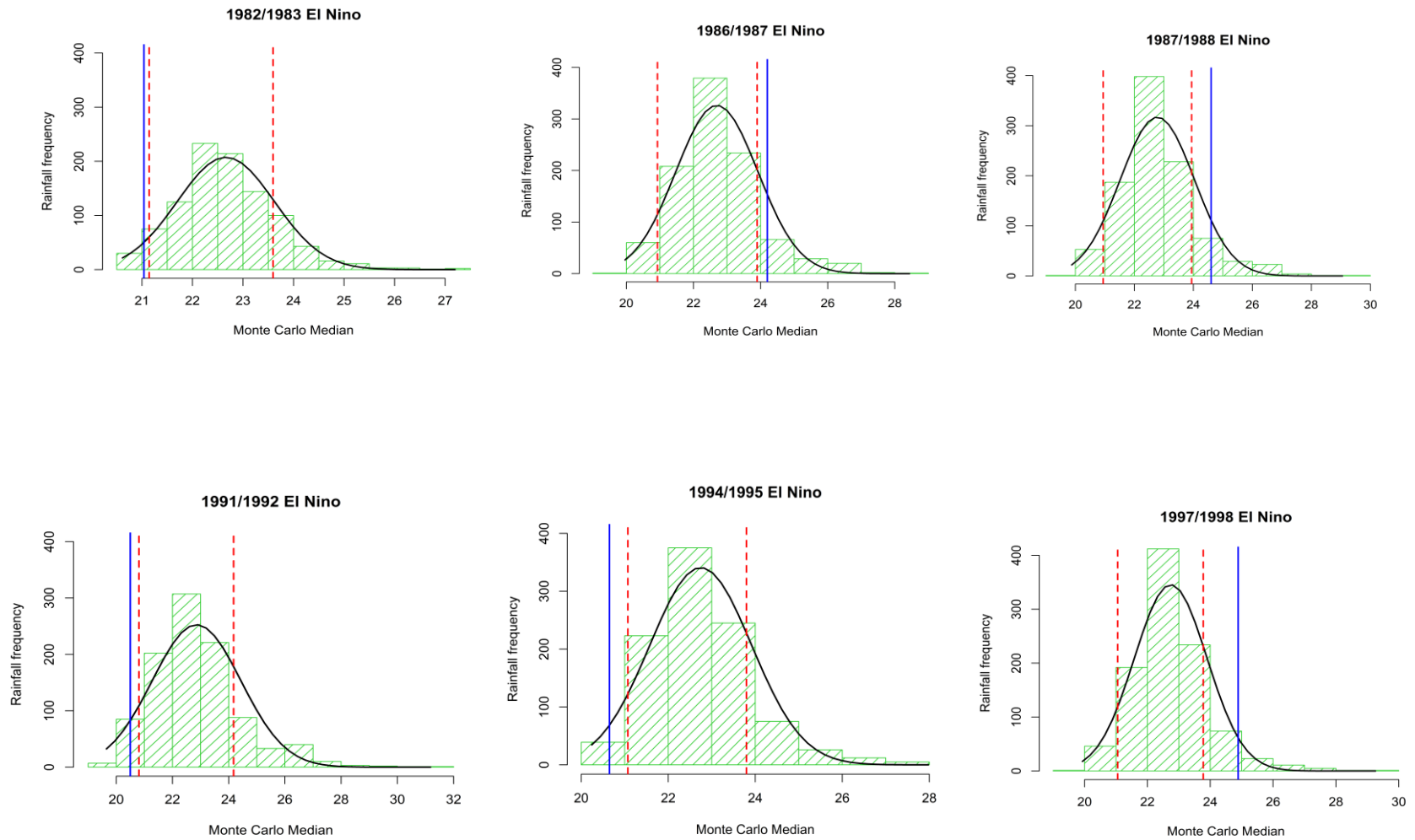


Figure 14: Significance test results for Bungoma station from Monte Carlo Simulations for daily rainfall above 95<sup>th</sup> Percentile.

The red dashed lines represent the 5<sup>th</sup> and 95<sup>th</sup> percentiles while the blue continuous line represent the Monte Carlo median

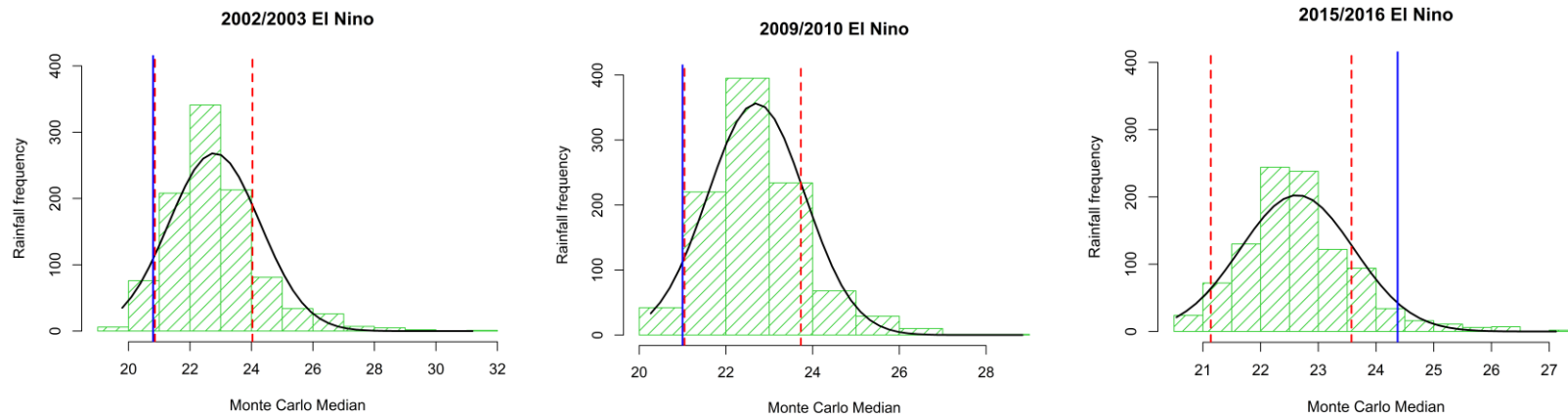


Figure 15: Significance test results for Bungoma station from Monte Carlo Simulations for daily rainfall above 95<sup>th</sup> Percentile. The red dashed lines represent the 5<sup>th</sup> and 95<sup>th</sup> percentiles while the blue continuous line represent the Monte Carlo median

#### 4.4 Objective 3 - Hydrological Modelling Results

For initial run, the GR4J model was set up with its default parametrization values indicated in Table 6 and run once with the precipitation data. The main goal of this was to determine the capacity of the GR4J model to replicate the overall hydrological conditions with the Nzoia basin. This was also vital to establish the baseline performance which would allow the assessment of the improvement gotten through calibration.

*Table 6: GR4J Model parameters setting*

<b>Model Parameter</b>	<b>Description</b>	<b>Optimal value</b>
X1	Production store maximum capacity	62.92
X2	Groundwater exchange coefficient (mm)	-12.84
X3	Routing store maximum capacity (one day ahead (mm))	875.12
X4	Unit Hydrograph Time base UH1 (days)	2.33

After establishing the baseline performance, the data was then divided into years for calibration and validation indicated in Table 7.

Table 7 below outlines the specific periods for calibration and validation within the GR4J model, including warm-up periods to establish and test the model's performance. Calibration Warm-Up Period (1981) allowed the model to stabilize and adjust initial settings without considering the data for calibration.

*Table 7: GR4J Calibration/Validation sub periods*

<b>Calibration Warm up Period</b>	<b>Calibration Period</b>	<b>Validation Warm up Period</b>	<b>Validation Period</b>
1981	1982 – 2000	2001	2002 – 2018

It basically sets the starting conditions for the calibration period. Calibration Period (1982-2000) involved modification of the model using observed data from 1982 to 2000. The model parameters are adjusted to best match the historical data during this time frame mainly to ensure that the model adequately captures the system's behavior and dynamics within this specific period. Validation Warm-Up Period (2001) allows the model to adjust to the conditions of the validation period, preparing it for making predictions without using the subsequent validation data. Validation Period (2002-2018) is an independent test of the model's performance.

*Table 8: Applied metrics results for the GR4J model*

<b>Model</b>	<b>Phase</b>	<b>NSE (%)</b>
GR4J	Calibration	72%
	Validation	61%

The applied metrics for evaluating the GR4J performance is presented in. The model demonstrates a generally better performance as indicated by the NSE values exceeding 50% during both the calibration and validation periods. The Nash-Sutcliffe efficiency, a widely used metric for assessing the accuracy of models, with values above 50% indicating an acceptable level of performance. However, there exists a disparity between the calibration and validation phases in terms of general model performance.

Calibration involves adjusting model parameters to best fit historical data. A 72% efficiency indicates that the model replicates the observed behavior of the system during the calibration period. Validation involves testing the model's performance on an independent dataset, typically a different time period from the calibration data. A NSE of 61% during validation indicates how well the model predicts unseen data.

*Table 9: Summary of the statistical characteristics of the basin observations*

<b>Summary</b>	<b>PET (mm)</b>	<b>Q obs(m<sup>3</sup>/sec)</b>	<b>Rainfall (mm)</b>	<b>Q obs (mm)</b>
Minimum	0.9	4.68	0	0.1
1 <sup>st</sup> Quartile	3.1	54.40	0.2	0.4
Median	3.6	109.10	1.8	0.7
Mean	3.7	133.36	4.1	1.1
3 <sup>rd</sup> Quartile	4.2	194.90	5.8	1.4
Maximum	6.6	611.87	50.2	4.2

The model is seen to perform better during the calibration phase in comparison to the validation phase. Analyzing the optimization criteria of the model provides valuable insights into the model's flood simulation ability over the basin. The optimization criteria serve as indicators for evaluating and appreciating the performance of the GR4J model. Other studies like Kodja et al., 2018 in an attempt to analyze the GR4J performance in reproducing high flows in similar also used the same criteria. These criteria helped in assessing how well the model captures the observed flood flows and how accurately it reproduces the dynamics of the basin's hydrological processes.

#### **4.4.1 GR4J Model Performance**

From the results (Figure 16 and 17), the observed and simulated flows depict a similar pattern with rainfall variability over the basin. Nonetheless, there exists a small bias between the observed and simulated flows that can be ascribed to most likely a slow response of the catchment basin to extreme rainfall events especially during the ENSO years. This slow response could arise due to model simplifications in accounting for slow water movement during extreme events, inadequate representation of soil saturation effects, or limitations in capturing the complexities of how the basin responds to heightened precipitation. However, the extreme rainfall events which cause flooding in the area, occur during these months depending on the season. Unfortunately, the heavy rainfall events which leads to basin flooding normally take place during these months depending on the season.

Further analysis on the simulated flows also shows an over estimation of the river flows during the low water period compared to the high water. The scatter plots of the observed verses simulated flows also depicted in Figure 16 and 17 for both the calibration and validation stages shows that the model slightly overestimates the simulation for higher flows during the validation phase while capturing higher ones with lower deviances during the calibration phase. From this, it is clear that the model performed better during the calibration phase compared to the validation. Similar findings were also realized in flood modelling in similar basins by Cantoni et al., 2022 using the GR4J model. Based on these findings, it is worth noting that the GR4J model generally represents well the average flows within the Nzoia River basin.

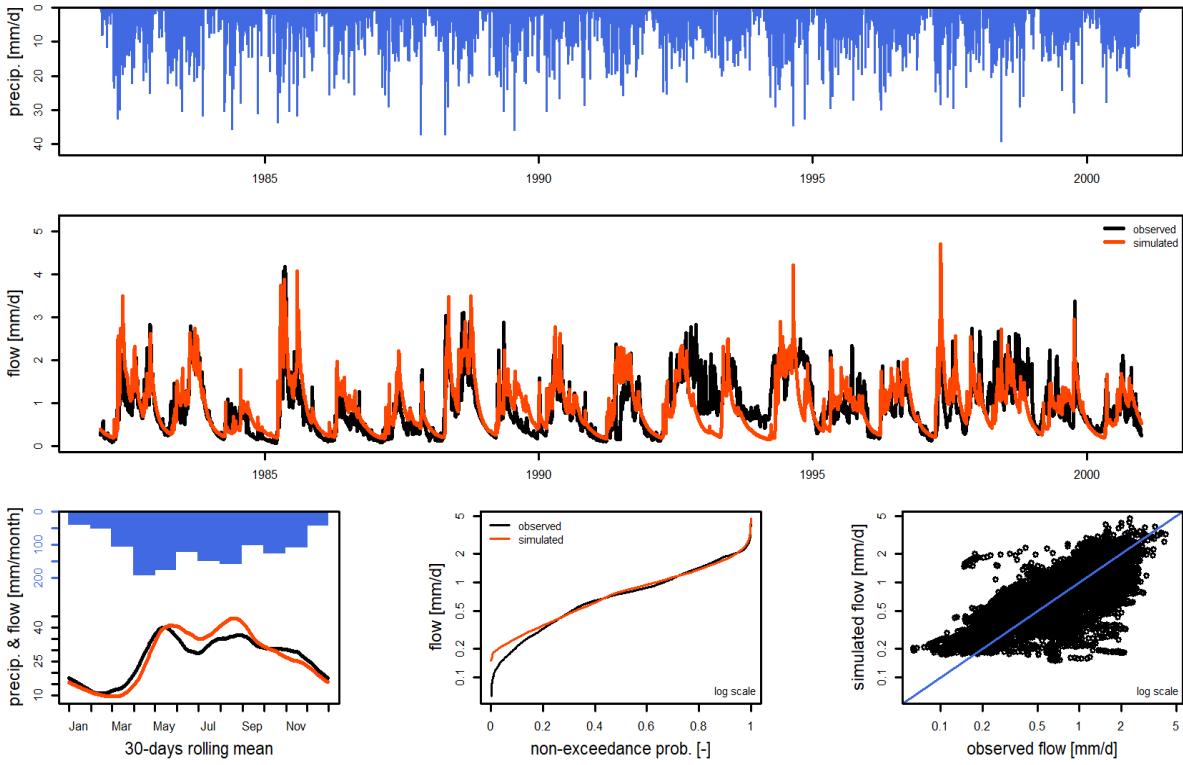


Figure 16: Rainfall variability, observed and simulated flow rates in calibration (1981-2006) with the GR4J model from the criterion of  $(NSE(Q))$

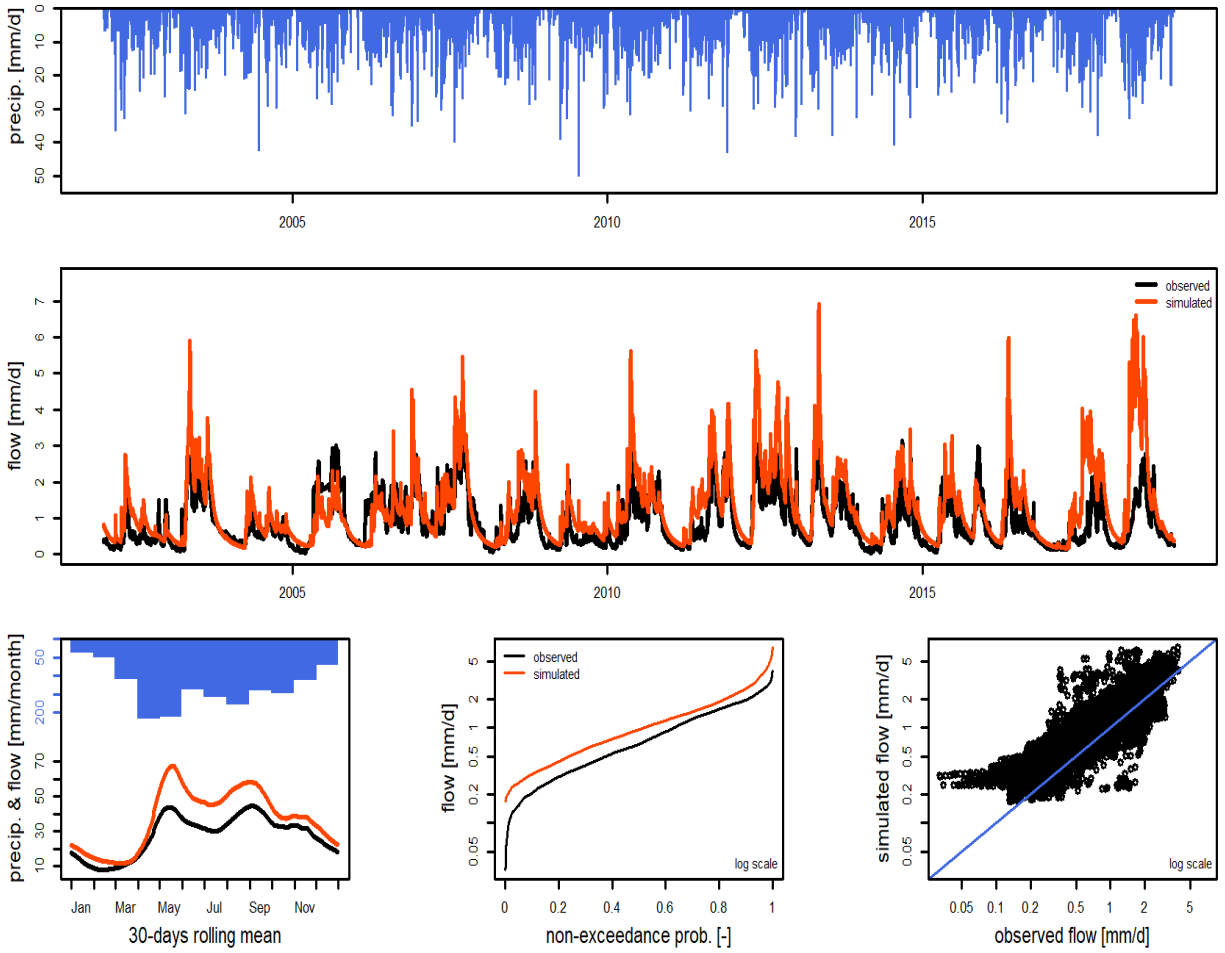


Figure 17: Rainfall variability, observed and simulated flow rates in validation (2007-2021) with the GR4J model from the criterion of  $(NSE(Q))$



## CHAPTER FIVE

### 5 SUMMARY, CONCLUSIONS AND RECOMMENDATIONS

#### 5.1 Summary

From the above analysis, trends in rainfall patterns over time, such as increasing or decreasing rainfall amounts were identified. The OND season rainfall variability depicts a slightly higher variations are found compared to the annual values. A range of variability of between 35% to 37% concentrates around the eastern parts of the basin area suggesting a less dependable rainfall during this season in this region. However, lower variability range of around 34% to 35% is seen more on the western parts mostly around the Mt. Elgon area indicating a relatively more dependable rainfall distribution during the OND season in these areas. The high OND rainfall variability compared to the annual variability suggest a less occurrence of rainfall during OND compared to the annual distribution.

Further analysis also identified the interannual variability of rainfall from year to year, which can be useful in understanding the impacts of flood events and will provide valuable insights for environmental management and planning.

ENSO – daily rainfall relationship results showed a greater variability in the extreme daily rainfall response (95<sup>th</sup> Percentile) to strong El Nino events in comparison with the daily rainfall greater than 1mm. Further results also indicated that during some strong El Nino events, slightly less intense rainfall events were experienced within the basin.

Hydrological modelling simulations showed that the observed and simulated flows have a similar pattern with rainfall variability over the basin except for a small bias that could be ascribed to either the response time of the catchment to extreme rainfall events especially during the ENSO years. The GR4J model showed a better performance with the Nash-Sutcliffe criterion (NSE) outcome values indicating an acceptable performance of above 50% both during the calibration and validation period. Even though there was a difference amongst the calibration and validation phases, the GR4J acquires higher performance during the calibration phase hence could be efficient to perform and reproduce high river flows in the basin.

## **5.2 Conclusions**

ENSO – flooding analysis can provide valuable insights on the connection between extreme weather events and various climate patterns. The findings would therefore be vital in informing flood management and preparedness, and hence build more resilient communities in flood-prone areas.

The study findings enhance the existing knowledge on ENSO impacts on extreme rainfall and flooding and provide a foundation for routine provision of sub-seasonal to seasonal flood forecasts. This, in the long run is expected to contribute considerably to a better management and sustainable growth of socio-economic activities which have been greatly impacted by floods over the years.

## **5.3 Recommendations**

A significant statistical relationship between ENSO and flooding in Nzoia River basin have been identified. This information can be used to inform flood forecasting EWS systems. Overall, this ENSO – flooding analysis can provide valuable insights on the connection between extreme weather events and various climate patterns. Policy makers and various stakeholders could incorporate the findings from this study to have in place measures to help the population cushion against expected risks that would result from extreme rainfall in the basin

The findings would therefore be vital in informing flood management and preparedness, and hence build more resilient communities in flood-prone areas within the Nzoia Basin and the larger western Kenya.

### **5.3.1 Research Scientists and Research Institutions**

Research scientists and institutions involved in climate and hydrology studies could leverage the identified statistical relationship between ENSO and flooding in the Nzoia River basin to enhance flood forecasting and Early Warning Systems (EWS). Further research could improve the accuracy and lead time of flood predictions in the basin. Collaborative efforts among research institutions would be beneficial for robust data collection, modeling, and dissemination of findings.

### **5.3.2 Policy makers**

Policy makers could incorporate the findings from this study into flood management strategies. These insights should inform the development and implementation of policies aimed at enhancing flood preparedness, response, and recovery in the Nzoia Basin and surrounding areas. Investment in infrastructure, early warning systems, community awareness programs, and disaster response mechanisms aligned with the forecasted risks would significantly mitigate the adverse impacts of extreme rainfall events. Incorporating scientific data into policy frameworks would contribute to building resilient communities in flood-prone regions and foster sustainable development.

### **5.3.3 Users of Climate/Flooding/Modeling Information:**

The findings from this study can be useful to the users relying on climate, flooding, and modeling information, such as emergency responders, local authorities, NGOs, and community leaders. They can use the findings to refine existing disaster preparedness plans, tailor educational campaigns, and implement proactive measures. Accessible dissemination of accurate, up-to-date information regarding potential flood risks linked to ENSO phases would empower communities to take timely actions, from implementing adaptive land-use practices to organizing evacuation plans. Encouraging the incorporation of these insights into decision-making processes at various levels would amplify the effectiveness of response measures and contribute to community resilience.

## REFERENCES

- Abram, N. J., Wright, N. M., Ellis, B., Dixon, B. C., Wurtzel, J. B., England, M. H., Ummenhofer, C. C., Philibosian, B., Cahyarini, S. Y., Yu, T. L., Shen, C. C., Cheng, H., Edwards, R. L., & Heslop, D. (2020). Coupling of Indo-Pacific climate variability over the last millennium. *Nature*, *579*(7799), 385–392. <https://doi.org/10.1038/s41586-020-2084-4>
- AfDB. (2014). AfDB. *Department, Africa Food Security Statistics*, *5*, 1–20.
- Alfieri, L., Burek, P., Dutra, E., Krzeminski, B., Muraro, D., Thielen, J., & Pappenberger, F. (2013). GloFAS-global ensemble streamflow forecasting and flood early warning. *Hydrology and Earth System Sciences*, *17*(3), 1161–1175. <https://doi.org/10.5194/hess-17-1161-2013>
- Ambrosino, C., Chandler, R. E., & Todd, M. C. (2011). Southern African monthly rainfall variability: An analysis based on generalized linear models. *Journal of Climate*, *24*(17), 4600–4617. <https://doi.org/10.1175/2010JCLI3924.1>
- Aming, P., Awange, J. L., Forootan, E., & Ogallo, A. (2014). *Changes in temperature and precipitation extremes over the Greater Horn of Africa region from 1961 to 2010. March 2018*. <https://doi.org/10.1002/joc.3763>
- Anderson, W. B., Seager, R., Baethgen, W., Cane, M., & You, L. (2019). Synchronous crop failures and climate-forced production variability. *Science Advances*, *5*(7), 1–10. <https://doi.org/10.1126/sciadv.aaw1976>
- Ash, K. D., & Matyas, C. J. (2012). The influences of ENSO and the subtropical Indian Ocean Dipole on tropical cyclone trajectories in the southwestern Indian Ocean. *International Journal of Climatology*, *32*(1), 41–56. <https://doi.org/10.1002/joc.2249>
- Ayugi, B. O., Tan, G., Ongoma, V., & Mafuru, K. B. (2018). Circulations Associated with Variations in Boreal Spring Rainfall over Kenya. *Earth Systems and Environment*, *2*(2), 421–434. <https://doi.org/10.1007/s41748-018-0074-6>

- Ayugi, B., Tan, G., Niu, R., Dong, Z., Ojara, M., Mumo, L., Babaousmail, H., & Ongoma, V. (n.d.). *Evaluation of Meteorological Drought and Flood Scenarios over Kenya , East Africa*.
- Bahaga, T. K., Mengistu Tsidu, G., Kucharski, F., & Diro, G. T. (2015). Potential predictability of the sea-surface temperature forced equatorial east african short rains interannual variability in the 20th century. *Quarterly Journal of the Royal Meteorological Society*, *141*(686), 16–26. <https://doi.org/10.1002/qj.2338>
- Barasa, B. N., & Perera, E. D. P. (2018). Analysis of land use change impacts on flash flood occurrences in the Sosiani River basin Kenya. *International Journal of River Basin Management*, *16*(2), 179–188. <https://doi.org/10.1080/15715124.2017.1411922>
- Bates, P. D., Horritt, M. S., & Fewtrell, T. J. (2010). A simple inertial formulation of the shallow water equations for efficient two-dimensional flood inundation modelling. *Journal of Hydrology*, *387*(1–2), 33–45. <https://doi.org/10.1016/j.jhydrol.2010.03.027>
- Berhane, F., & Zaitchik, B. (2014). Modulation of daily precipitation over East Africa by the Madden-Julian oscillation. *Journal of Climate*, *27*(15), 6016–6034. <https://doi.org/10.1175/JCLI-D-13-00693.1>
- Beyene, T., Lettenmaier, D. P., & Kabat, P. (2010). Hydrologic impacts of climate change on the Nile River Basin: Implications of the 2007 IPCC scenarios. *Climatic Change*, *100*(3), 433–461. <https://doi.org/10.1007/s10584-009-9693-0>
- Bizimana, J.-C., Bessler Regents, D. A., & Angerer, J. P. (2016). The 2010-2011 Drought Impacts on Cattle Market Integration in the Horn of Africa: A preliminary Evaluation using VAR and Structural Break Analysis. *Paper Presented at the Southern Agricultural Economics Association Annual Meeting*, 1–26.
- Bliss, M., Teklu, D., Rafael, R., & Cut, M. O. (2021). *Data Descriptor Hourly potential evapotranspiration at 0.1 ° resolution for the global land surface from 1981-present*. 1–13. <https://doi.org/10.1038/s41597-021-01003-9>
- Byrne, M. P., & Schneider, T. (2016). Narrowing of the ITCZ in a warming climate: Physical mechanisms. *Geophysical Research Letters*, *43*(21), 11,350-11,357.

<https://doi.org/10.1002/2016GL070396>

- Cai, W., Borlace, S., Lengaigne, M., Van Rensch, P., Collins, M., Vecchi, G., Timmermann, A., Santoso, A., Mcphaden, M. J., Wu, L., England, M. H., Wang, G., Guilyardi, E., & Jin, F. F. (2014). Increasing frequency of extreme El Niño events due to greenhouse warming. *Nature Climate Change*, 4(2), 111–116. <https://doi.org/10.1038/nclimate2100>
- Cai, W., Van Rensch, P., Cowan, T., & Hendon, H. H. (2012). An Asymmetry in the IOD and ENSO teleconnection pathway and its impact on australian climate. *Journal of Climate*, 25(18), 6318–6329. <https://doi.org/10.1175/JCLI-D-11-00501.1>
- Cai, W., Wang, G., Santoso, A., Mcphaden, M. J., Wu, L., Jin, F. F., Timmermann, A., Collins, M., Vecchi, G., Lengaigne, M., England, M. H., Dommenges, D., Takahashi, K., & Guilyardi, E. (2015). Increased frequency of extreme La Niña events under greenhouse warming. *Nature Climate Change*, 5(2), 132–137. <https://doi.org/10.1038/nclimate2492>
- Camberlin, P., Fontaine, B., Louvet, S., Oettli, P., & Valimba, P. (2010). Climate adjustments over Africa accompanying the Indian monsoon onset. *Journal of Climate*, 23(8), 2047–2064. <https://doi.org/10.1175/2009JCLI3302.1>
- Cantoni, E., Trambly, Y., Grimaldi, S., Salamon, P., Dakhlaoui, H., Dezetter, A., & Thiemi, V. (2022). Hydrological performance of the ERA5 reanalysis for flood modeling in Tunisia with the LISFLOOD and GR4J models. *Journal of Hydrology: Regional Studies*, 42(July), 101169. <https://doi.org/10.1016/j.ejrh.2022.101169>
- Cattani, E., Merino, A., Guijarro, J. A., & Levizzani, V. (2018). East Africa Rainfall trends and variability 1983-2015 using three long-term satellite products. *Remote Sensing*, 10(6), 1–26. <https://doi.org/10.3390/rs10060931>
- Conway, D., Allison, E., Felstead, R., & Goulden, M. (2005). Rainfall variability in East Africa: Implications for natural resources management and livelihoods. *Philosophical Transactions of the Royal Society A: Mathematical, Physical and Engineering Sciences*, 363(1826), 49–54. <https://doi.org/10.1098/rsta.2004.1475>
- CRED. (2019). Disasters 2018: Year in Review. *PLoS ONE*, 14(3), 2018–2019.

[https://www.preventionweb.net/files/65061\\_credcrunch54.pdf](https://www.preventionweb.net/files/65061_credcrunch54.pdf)

- Diro, G. T., Grimes, D. I. F., & Black, E. (2011). Teleconnections between Ethiopian summer rainfall and sea surface temperature: Part I-observation and modelling. *Climate Dynamics*, 37(1), 103–119. <https://doi.org/10.1007/s00382-010-0837-8>
- Edijatno, De Oliveira Nascimento, N., Yang, X., Makhlof, Z., & Michel, C. (1999). GR3J: A daily watershed model with three free parameters. *Hydrological Sciences Journal*, 44(2), 263–277. <https://doi.org/10.1080/02626669909492221>
- Emerton, R., Zsoter, E., Arnal, L., Cloke, H. L., Muraro, D., Prudhomme, C., Stephens, E. M., Salamon, P., & Pappenberger, F. (2018). Developing a global operational seasonal hydro-meteorological forecasting system: GloFAS-Seasonal v1.0. *Geoscientific Model Development*, 11(8), 3327–3346. <https://doi.org/10.5194/gmd-11-3327-2018>
- Endris, H. S., Lennard, C., Hewitson, B., Dosio, A., Nikulin, G., & Artan, G. A. (2019). Future changes in rainfall associated with ENSO, IOD and changes in the mean state over Eastern Africa. *Climate Dynamics*, 52(3–4), 2029–2053. <https://doi.org/10.1007/s00382-018-4239-7>
- Enfield, D. B., & Mestas-núñez, A. M. (2010). Global Modes of ENSO and Non-ENSO Sea Surface Temperature Variability and Their Associations with Climate. *El Nino and the Southern Oscillation*, 89–112. <https://doi.org/10.1017/cbo9780511573125.004>
- Ficchì, A., Perrin, C., & Andréassian, V. (2019). Hydrological modelling at multiple sub-daily time steps: Model improvement via flux-matching. *Journal of Hydrology*, 575, 1308–1327. <https://doi.org/10.1016/j.jhydrol.2019.05.084>
- Findlater, J. (1977). Observational aspects of the low-level cross-equatorial jet stream of the western Indian Ocean. *Pure and Applied Geophysics PAGEOPH*, 115(5–6), 1251–1262. <https://doi.org/10.1007/BF00874408>
- Funk, C., Hoell, A., Shukla, S., Bladé, I., Liebmann, B., Roberts, J. B., Robertson, F. R., & Husak, G. (2014). Predicting East African spring droughts using Pacific and Indian Ocean sea surface temperature indices. *Hydrology and Earth System Sciences*, 18(12), 4965–4978. <https://doi.org/10.5194/hess-18-4965-2014>

- Funk, Chris, Dettinger, M. D., Michaelsen, J. C., Verdin, J. P., Brown, M. E., Barlow, M., & Hoell, A. (2008). Warming of the Indian Ocean threatens eastern and southern African food security but could be mitigated by agricultural development. *Proceedings of the National Academy of Sciences of the United States of America*, 105(32), 11081–11086. <https://doi.org/10.1073/pnas.0708196105>
- Funk, Chris, Peterson, P., Landsfeld, M., Pedreros, D., Verdin, J., Shukla, S., Husak, G., Rowland, J., Harrison, L., Hoell, A., & Michaelsen, J. (2015). The climate hazards infrared precipitation with stations - A new environmental record for monitoring extremes. *Scientific Data*, 2, 1–21. <https://doi.org/10.1038/sdata.2015.66>
- Gannon, K. E., Conway, D., Pardoe, J., Ndiyoi, M., Batisani, N., Odada, E., Olago, D., Opere, A., Kgosietsile, S., Nyambe, M., Omukuti, J., & Siderius, C. (2018). Business experience of floods and drought-related water and electricity supply disruption in three cities in sub-Saharan Africa during the 2015/2016 El Niño. *Global Sustainability*, 1. <https://doi.org/10.1017/sus.2018.14>
- Geen, R., Bordoni, S., Battisti, D. S., & Hui, K. (2020). Monsoons, ITCZs, and the Concept of the Global Monsoon. *Reviews of Geophysics*, 58(4), 1–60. <https://doi.org/10.1029/2020RG000700>
- Giannini, A. (2010). *The Influence of Sea Surface Temperatures on African Climate*. September, 6–9.
- Giannini, A., Biasutti, M., Held, I. M., & Sobel, A. H. (2008). A global perspective on African climate. *Climatic Change*, 90(4), 359–383. <https://doi.org/10.1007/s10584-008-9396-y>
- Goddard, L., & Mason, S. (2002). Sensitivity of seasonal climate forecasts to persisted SST anomalies. *Climate Dynamics*, 19(7), 619–631. <https://doi.org/10.1007/s00382-002-0251-y>
- Goddard, Lisa, & Graham, E. (1999). *anomalies I / i / . 104*.
- Hameed, S. N., Jin, D., & Thilakan, V. (2018). A model for super El Niños. *Nature Communications*, 9(1), 1–15. <https://doi.org/10.1038/s41467-018-04803-7>



- Hashizume, M., Chaves, L. F., & Minakawa, N. (2012). Indian Ocean Dipole drives malaria resurgence in East African highlands. *Scientific Reports*, 2, 1–6. <https://doi.org/10.1038/srep00269>
- Hong, C. hoon, Cho, K. D., & Kim, H. J. (2001). The relationship between ENSO events and sea surface temperature in the east (Japan) sea. *Progress in Oceanography*, 49(1–4), 21–40. [https://doi.org/10.1016/S0079-6611\(01\)00014-3](https://doi.org/10.1016/S0079-6611(01)00014-3)
- Indeje, M., & Semazzi, F. H. M. (2000). Enso signals in East African Rainfall seasons. *International journal of Climatology*, 20, 19-46. doi:10.1002/(SICI)1097-0088(200001)20:1<19::AID-JOC449>3.0.CO;2-0, [http://dx.doi.org/10.1002/\(SICI\)1097-0088](http://dx.doi.org/10.1002/(SICI)1097-0088). *International Journal of Climatology*, 46, 19–46.
- Jane Kabubo-Mari ara, & Kabara, M. l l i cent. (2015). *Environment for Development Centers Climate Change and Food Security in Kenya*. 1–36.
- Joshua, N., James, N., Francis, M., Bethwel, M., & Alfred, O. (2014). *Flood Forecasting over Lower Nzoia Sub-Basin in Kenya*. 1(1).
- Kamau, J., Ngisiange, N., Ochola, O., Kilionzi, J., Kimeli, A., Mahongo, S. B., Onganda, H., Mitto, C., Ohowa, B., Magori, C., Kimani, E., & Osore, M. (2020). Factors influencing spatial patterns in primary productivity in Kenyan territorial waters. *Western Indian Ocean Journal of Marine Science*, 2020(1 Special Issue), 9–18. <https://doi.org/10.4314/wiojms.si2020.1.2>
- Kandji, S. T., Verchot, L. V, Fertility, S., & Change, C. (2006). Impacts of and Adaptation to Climate Variability and Climate Change in the East African Community A Focus on the Agricultural Sector. *Change*.
- Kilavi, M., MacLeod, D., Ambani, M., Robbins, J., Dankers, R., Graham, R., Helen, T., Salih, A. A. M., & Todd, M. C. (2018). Extreme rainfall and flooding over Central Kenya Including Nairobi City during the long-rains season 2018: Causes, predictability, and potential for early warning and actions. *Atmosphere*, 9(12). <https://doi.org/10.3390/atmos9120472>
- King, J. A., Engelstaedter, S., Washington, R., & Munday, C. (2021). Variability of the Turkana Low-Level Jet in Reanalysis and Models: Implications for Rainfall. *Journal of Geophysical*

*Research: Atmospheres*, 126(10), 1–24. <https://doi.org/10.1029/2020JD034154>

Klotzbach, P., Blake, E., Camp, J., Caron, L.-P., Chan, J. C. L., Kang, N.-Y., Kuleshov, Y., Lee, S.-M., Murakami, H., Saunders, M., Takaya, Y., Vitart, F., & Zhan, R. (2019). Seasonal Tropical Cyclone Forecasting. *Tropical Cyclone Research and Review*, 8(3), 134–149. <https://doi.org/10.1016/j.tcr.2019.10.003>

Klotzbach, P. J., & Oliver, E. C. J. (2015). Variations in global tropical cyclone activity and the Madden-Julian Oscillation since the midtwentieth century. *Geophysical Research Letters*, 42(10), 4199–4207. <https://doi.org/10.1002/2015GL063966>

Kodja, D. J., Mahé, G., Amoussou, E., Boko, M., & Paturel, J.-E. (2018). Assessment of the Performance of Rainfall-Runoff Model GR4J to Simulate Streamflow in Ouémé Watershed at Bonou's outlet (West Africa). *Preprint, March*, 18. <https://doi.org/10.20944/preprints201803.0090.v1>

Korecha, D., & Barnston, A. G. (2007). Predictability of June-September rainfall in Ethiopia. *Monthly Weather Review*, 135(2), 628–650. <https://doi.org/10.1175/MWR3304.1>

Kousky, V. E., & Higgins, R. W. (2007). An alert classification system for monitoring and assessing the ENSO cycle. *Weather and Forecasting*, 22(2), 353–371. <https://doi.org/10.1175/WAF987.1>

Krysanova, V., Vetter, T., Eisner, S., Huang, S., Pechlivanidis, I., Strauch, M., Gelfan, A., Kumar, R., Aich, V., Arheimer, B., Chamorro, A., Van Griensven, A., Kundu, D., Lobanova, A., Mishra, V., Plötner, S., Reinhardt, J., Seidou, O., Wang, X., ... Hattermann, F. F. (2017). Intercomparison of regional-scale hydrological models and climate change impacts projected for 12 large river basins worldwide - A synthesis. *Environmental Research Letters*, 12(10). <https://doi.org/10.1088/1748-9326/aa8359>

Lau, N. C., Leetmaa, A., & Nath, M. J. (2008). Interactions between the responses of North American climate to El Niño-La Niña and to the secular warming trend in the India-Western Pacific Oceans. *Journal of Climate*, 21(3), 476–494. <https://doi.org/10.1175/2007JCLI1899.1>

Le, A. M., & Pricope, N. G. (2017). *Increasing the Accuracy of Runoff and Streamflow*. *March*

2021. <https://doi.org/10.3390/w9020114>

- Liebmann, B., Bladé, I., Funk, C., Allured, D., Quan, X. W., Hoerling, M., Hoell, A., Peterson, P., & Thiaw, W. M. (2017). Climatology and interannual variability of boreal spring wet season precipitation in the eastern horn of Africa and implications for its recent decline. *Journal of Climate*, *30*(10), 3867–3886. <https://doi.org/10.1175/JCLI-D-16-0452.1>
- Lim, E. P., Hendon, H. H., Zhao, M., & Yin, Y. (2017). Inter-decadal variations in the linkages between ENSO, the IOD and south-eastern Australian springtime rainfall in the past 30 years. *Climate Dynamics*, *49*(1–2), 97–112. <https://doi.org/10.1007/s00382-016-3328-8>
- Liu, C., Liao, X., Qiu, J., Yang, Y., Feng, X., Allan, R. P., Cao, N., Long, J., & Xu, J. (2020). Observed variability of intertropical convergence zone over 1998-2018. *Environmental Research Letters*, *15*(10). <https://doi.org/10.1088/1748-9326/aba033>
- Lyon, B. (2014). Seasonal drought in the Greater Horn of Africa and its recent increase during the March-May long rains. *Journal of Climate*, *27*(21), 7953–7975. <https://doi.org/10.1175/JCLI-D-13-00459.1>
- Lyon, B., & Dewitt, D. G. (2012). A recent and abrupt decline in the East African long rains. *Geophysical Research Letters*, *39*(2), 1–5. <https://doi.org/10.1029/2011GL050337>
- M. V. Subrahmanyam, B. P. (2014). Sea Surface Temperature and Find Later Jet Variations over Arabian Sea During Summer Monsoon. *Journal of Climatology & Weather Forecasting*, *02*(02), 1–5. <https://doi.org/10.4172/2332-2594.1000111>
- Macleod, D. A., Dankers, R., Graham, R., Guigma, K., Jenkins, L., Todd, M. C., Kiptum, A., Kilavi, M., Njogu, A., & Mwangi, E. (2021). Drivers and subseasonal predictability of heavy rainfall in equatorial east africa and relationship with flood risk. *Journal of Hydrometeorology*, *22*(4), 887–903. <https://doi.org/10.1175/JHM-D-20-0211.1>
- Macleod, D., & Caminade, C. (2019). The moderate impact of the 2015 El Niño over East Africa and its representation in seasonal reforecasts. *Journal of Climate*, *32*(22), 7989–8001. <https://doi.org/10.1175/JCLI-D-19-0201.1>

- Madden, R. A., & Julian, P. R. (1971). Detection of a 40–50 Day Oscillation in the Zonal Wind in the Tropical Pacific. In *Journal of the Atmospheric Sciences* (Vol. 28, Issue 5, pp. 702–708). [https://doi.org/10.1175/1520-0469\(1971\)028<0702:doadoi>2.0.co;2](https://doi.org/10.1175/1520-0469(1971)028<0702:doadoi>2.0.co;2)
- Manatsa, D., Morioka, Y., Behera, S. K., Matarira, C. H., & Yamagata, T. (2014). Impact of Mascarene High variability on the East African “short rains.” *Climate Dynamics*, 42(5–6), 1259–1274. <https://doi.org/10.1007/s00382-013-1848-z>
- Melsen, L. A., Teuling, A. J., Torfs, P. J. J. F., Zappa, M., Mizukami, N., Mendoza, P. A., Clark, M. P., & Uijlenhoet, R. (2019). Subjective modeling decisions can significantly impact the simulation of flood and drought events. *Journal of Hydrology*, 568(November 2018), 1093–1104. <https://doi.org/10.1016/j.jhydrol.2018.11.046>
- Mukabana, J. R. (1992). *Numerical Simulation of the Influences of the Large-Scale Monsoon Flow on the Diurnal Weather Patterns over Kenya*. 225.
- Mutai, C. C., & Ward, M. N. (2000). East African rainfall and the tropical circulation/convection on intraseasonal to interannual timescales. *Journal of Climate*, 13(22), 3915–3939. [https://doi.org/10.1175/1520-0442\(2000\)013<3915:EARATT>2.0.CO;2](https://doi.org/10.1175/1520-0442(2000)013<3915:EARATT>2.0.CO;2)
- Mutai, C. C., Ward, M. N., & Colman, A. W. (1998). Towards the prediction of the East Africa short rains based on sea-surface temperature-atmosphere coupling. *International Journal of Climatology*, 18(9), 975–997. [https://doi.org/10.1002/\(sici\)1097-0088\(199807\)18:9<975::aid-joc259>3.0.co;2-u](https://doi.org/10.1002/(sici)1097-0088(199807)18:9<975::aid-joc259>3.0.co;2-u)
- Mutemi, J. N., Ogallo, L. A., Krishnamurti, T. N., Mishra, A. K., & Vijaya Kumar, T. S. V. (2007). Multimodel based superensemble forecasts for short and medium range NWP over various regions of Africa. *Meteorology and Atmospheric Physics*, 95(1–2), 87–113. <https://doi.org/10.1007/s00703-006-0187-6>
- Nash, J. E., & Sutcliffe, J. V. (1970). River Flow Forecasting Through Conceptual Models - Part I - A Discussion of Principles. *Journal of Hydrology*, 10(1970), 282–290.
- Neumann, J. L., Arnal, L., Emerton, R. E., Griffith, H., Hyslop, S., Theofanidi, S., & Cloke, H. L. (2018). Can seasonal hydrological forecasts inform local decisions and actions? A decision-

- making activity. *Geoscience Communication*, 1(1), 35–57. <https://doi.org/10.5194/gc-1-35-2018>
- Ng'ongolo, H. K., & Smyshlyaev, S. P. (2010). The statistical prediction of East African rainfalls using quasi-biennial oscillation phases information. *Natural Science*, 02(12), 1407–1416. <https://doi.org/10.4236/ns.2010.212172>
- Nicholson, S. E. (2017). Climate and climatic variability of rainfall over eastern Africa. *Reviews of Geophysics*, 55(3), 590–635. <https://doi.org/10.1002/2016RG000544>
- Njogu, H. W. (2021). Effects of floods on infrastructure users in Kenya. *Journal of Flood Risk Management*, 14(4), 1–10. <https://doi.org/10.1111/jfr3.12746>
- Notification, P., Consultation, P., Land, E. U., Inspector, W. R., Data, W. R., Resource, W., Identification, U., Application, P., & Report, T. (2006). *Kenya Gazette Supplement No ( Legislative Supplement No ....) LEGAL NOTICE NO (.....) THE WATER RESOURCES MANAGEMENT RULES , 2006 ARRANGEMENTS OF RULES*. 1–74.
- Odwori, E. O., & Wakhungu, J. W. (2021). Analysis of Rainfall Variability and Trends Over Nzoia River Basin, Kenya. *Journal of Engineering Research and Reports*, 21(4), 26–52. <https://doi.org/10.9734/jerr/2021/v21i417457>
- Ogallo, L. J., Janowiak, J. E., & Halpert, M. S. (1988). Teleconnection between seasonal rainfall over East Africa and global sea surface temperature anomalies. *Journal of the Meteorological Society of Japan*, 66(6), 807–822. [https://doi.org/10.2151/jmsj1965.66.6\\_807](https://doi.org/10.2151/jmsj1965.66.6_807)
- Okoola, R. E. (1999). A diagnostic study of the eastern Africa monsoon circulation during the Northern Hemisphere spring season. *International Journal of Climatology*, 19(2), 143–168. [https://doi.org/10.1002/\(SICI\)1097-0088\(199902\)19:2<143::AID-JOC342>3.0.CO;2-U](https://doi.org/10.1002/(SICI)1097-0088(199902)19:2<143::AID-JOC342>3.0.CO;2-U)
- Olang, L. O., & Fürst, J. (2011). Effects of land cover change on flood peak discharges and runoff volumes: Model estimates for the Nyando River Basin, Kenya. *Hydrological Processes*, 25(1), 80–89. <https://doi.org/10.1002/hyp.7821>
- Olila, D. O., & Wasonga, V. O. (2016). *Nexus between Climate Change and Food security in the*

- East Africa Region: An Application of Autoregressive Modelling Approach. October, 17–21.*
- Omay, P. O., Christopher, O., & Atheru, Z. (2023). *Observed Changes and Variability in wet days and Dry Spells over IGAD region of Eastern Africa.*
- Omeny, P. A., Okoola, R., Hendon, H., & Wheeler, M. (2008). East African Rainfall Variability Associated with the Madden-Julian Oscillation LABAN OGALLO IGAD CLIMATE PREDICTION AND APPLICATIONS CENTRE, Nairobi (ICPAC). *J.Kenya Meteorol. Soc*, 2(2), 105–114. <http://www.cdc.noaa.gov>
- Omondi, P., Awange, J. L., Ogallo, L. A., Okoola, R. A., & Forootan, E. (2012). Decadal rainfall variability modes in observed rainfall records over East Africa and their relations to historical sea surface temperature changes. *Journal of Hydrology*, 464–465, 140–156. <https://doi.org/10.1016/j.jhydrol.2012.07.003>
- Omondi, Philip, Ogallo, L. A., Anyah, R., Muthama, J. M., & Ininda, J. (2013). Linkages between global sea surface temperatures and decadal rainfall variability over Eastern Africa region. *International Journal of Climatology*, 33(8), 2082–2104. <https://doi.org/10.1002/joc.3578>
- Ongoma, V., Guirong, T., Ogwang, B., & Ngarukiyimana, J. (2015). Diagnosis of Seasonal Rainfall Variability over East Africa: A Case Study of 2010-2011 Drought over Kenya. *Pakistan Journal of Meteorology*, 11(22), 13–21.
- Onyando, J. O., Schumann, A. H., & Schultz, G. A. (2003). Simulation of flood hydrographs based on lumped and semi-distributed models for two tropical catchments in Kenya. *Hydrological Sciences Journal*, 48(4), 511–524. <https://doi.org/10.1623/hysj.48.4.511.51411>
- Oscar, L., Nzau, M. J., Ellen, D., Franklin, O., Rachel, J., Richard, W., & Tom, W. (2022). Characteristics of the Turkana low-level jet stream and the associated rainfall in CMIP6 models. *Climate Dynamics*, 0123456789. <https://doi.org/10.1007/s00382-022-06499-4>
- Othieno, E. (2022). *Effect of Rainfall and Temperature Variability on Streamflow in Nzoia River Basin , Kenya. 16(5), 33–61.* <https://doi.org/10.9734/AJARR/2022/v16i530473>
- Otieno, V. O., & Anyah, R. O. (2013). CMIP5 simulated climate conditions of the Greater Horn

- of Africa (GHA). Part II: Projected climate. *Climate Dynamics*, 41(7–8), 2099–2113. <https://doi.org/10.1007/s00382-013-1694-z>
- Owuor, M. O., & Mwiturubani, D. A. (2022). Correlation between flooding and settlement planning in Nairobi. *Journal of Water and Climate Change*, 13(4), 1790–1805. <https://doi.org/10.2166/wcc.2022.335>
- Parajka, J., Viglione, A., Rogger, M., Salinas, J. L., Sivapalan, M., & Blöschl, G. (2013). Comparative assessment of predictions in ungauged basins-Part 1: Runoff-hydrograph studies. *Hydrology and Earth System Sciences*, 17(5), 1783–1795. <https://doi.org/10.5194/hess-17-1783-2013>
- Pascoe, C. L., Gray, L. J., Crooks, S. A., Jukes, M. N., & Baldwin, M. P. (2005). The quasi-biennial oscillation: Analysis using ERA-40 data. *Journal of Geophysical Research D: Atmospheres*, 110(8), 1–13. <https://doi.org/10.1029/2004JD004941>
- Paul, P. K., Kumari, B., Gaur, S., Mishra, A., Panigrahy, N., & Singh, R. (2020). Application of a newly developed large-scale conceptual hydrological model in simulating streamflow for credibility testing in data scarce condition. *Natural Resource Modeling*, 33(4), 1–27. <https://doi.org/10.1111/nrm.12283>
- Perrin, C., Michel, C., & Andréassian, V. (2003). Improvement of a parsimonious model for streamflow simulation. *Journal of Hydrology*, 279(1–4), 275–289. [https://doi.org/10.1016/S0022-1694\(03\)00225-7](https://doi.org/10.1016/S0022-1694(03)00225-7)
- Plisnier, P. D., Serneels, S., & Lambin, E. F. (2000). Impact of ENSO on East African ecosystems: A multivariate analysis based on climate and remote sensing data. *Global Ecology and Biogeography*, 9(6), 481–497. <https://doi.org/10.1046/j.1365-2699.2000.00208.x>
- Pohl, B., & Camberlin, P. (2006). Influence of the Madden-Julian Oscillation on East African rainfall. I: Intraseasonal variability and regional dependency. *Quarterly Journal of the Royal Meteorological Society*, 132(621), 2521–2539. <https://doi.org/10.1256/qj.05.104>
- Pricope, N. G., Husak, G., Lopez-Carr, D., Funk, C., & Michaelsen, J. (2013). The climate-population nexus in the East African Horn: Emerging degradation trends in rangeland and

- pastoral livelihood zones. *Global Environmental Change*, 23(6), 1525–1541. <https://doi.org/10.1016/j.gloenvcha.2013.10.002>
- Sandjon, A. T., Nzeukou, A., Tchawoua, C., Sonfack, B., & Siddi, T. (2014). Comparing the patterns of 20–70 days intraseasonal oscillations over Central Africa during the last three decades. *Theoretical and Applied Climatology*, 118(1–2), 319–329. <https://doi.org/10.1007/s00704-013-1063-1>
- Schreck, C. J., & Semazzi, F. H. M. (2004). Variability of the recent climate of eastern Africa. *International Journal of Climatology*, 24(6), 681–701. <https://doi.org/10.1002/joc.1019>
- Sciences, G. (2013). *Projected Changes in East African Rainy Seasons*. 5931–5948. <https://doi.org/10.1175/JCLI-D-12-00455.1>
- Serdeczny, O., Adams, S., Coumou, D., Hare, W., & Perrette, M. (2016). *repercussions. JANUARY*. <https://doi.org/10.1007/s10113-015-0910-2>
- Shongwe, M. E., van Oldenborgh, G. J., van den Hurk, B., & van Aalst, M. (2011). Projected changes in mean and extreme precipitation in Africa under global warming. Part II: East Africa. *Journal of Climate*, 24(14), 3718–3733. <https://doi.org/10.1175/2010JCLI2883.1>
- Shukla, S., McNally, A., Husak, G., & Funk, C. (2014). A seasonal agricultural drought forecast system for food-insecure regions of East Africa. *Hydrology and Earth System Sciences*, 18(10), 3907–3921. <https://doi.org/10.5194/hess-18-3907-2014>
- Stevenson, S., Baylor, F. K., Jochum, M., Neale, R., Deser, C., & Meehl, G. (2012). Will there be a significant change to El Niño in the twenty-first century? *Journal of Climate*, 25(6), 2129–2145. <https://doi.org/10.1175/JCLI-D-11-00252.1>
- Suzuki, T. (2011). Seasonal variation of the ITCZ and its characteristics over central Africa. *Theoretical and Applied Climatology*, 103(1), 39–60. <https://doi.org/10.1007/s00704-010-0276-9>
- Talha, S., Maanan, M., Atika, H., & Rhinane, H. (2019). PREDICTION of FLASH FLOOD SUSCEPTIBILITY USING FUZZY ANALYTICAL HIERARCHY PROCESS (FAHP)



- ALGORITHMS and GIS: A STUDY CASE of GUELMIM REGION in SOUTHWESTERN of MOROCCO. *International Archives of the Photogrammetry, Remote Sensing and Spatial Information Sciences - ISPRS Archives*, 42(4/W19), 407–414. <https://doi.org/10.5194/isprs-archives-XLII-4-W19-407-2019>
- Tempest, E. L., Carter, B., Beck, C. R., & Rubin, G. J. (2017). Secondary stressors are associated with probable psychological morbidity after flooding: A cross-sectional analysis. *European Journal of Public Health*, 27(6), 1042–1047. <https://doi.org/10.1093/eurpub/ckx182>
- Tierney, J. E., Ummenhofer, C. C., & DeMenocal, P. B. (2015). Past and future rainfall in the Horn of Africa. *Science Advances*, 1(9), 1–9. <https://doi.org/10.1126/sciadv.1500682>
- Trenberth, K. E. (1997). The Definition of El Niño. *Bulletin of the American Meteorological Society*, 78(12), 2771–2777. [https://doi.org/10.1175/1520-0477\(1997\)078<2771:TDOENO>2.0.CO;2](https://doi.org/10.1175/1520-0477(1997)078<2771:TDOENO>2.0.CO;2)
- Tyson, P. D., Edwards, M., & K, P. (1996). Southern Aerosols. *October*, 101.
- Ummenhofer, C. C., England, M. H., McIntosh, P. C., Meyers, G. A., Pook, M. J., Risbey, J. S., Gupta, A. Sen, & Taschetto, A. S. (2009). What causes southeast Australia’s worst droughts? *Geophysical Research Letters*, 36(4), 1–5. <https://doi.org/10.1029/2008GL036801>
- Verdin, J., Funk, C., Senay, G., & Choularton, R. (2005). Climate science and famine early warning. *Philosophical Transactions of the Royal Society B: Biological Sciences*, 360(1463), 2155–2168. <https://doi.org/10.1098/rstb.2005.1754>
- Vigaud, N., Lyon, B., & Giannini, A. (2017). Sub-seasonal teleconnections between convection over the Indian Ocean, the East African long rains and tropical Pacific surface temperatures. *International Journal of Climatology*, 37(3), 1167–1180. <https://doi.org/10.1002/joc.4765>
- Wainwright, C. M., Finney, D. L., Kilavi, M., Black, E., & Marsham, J. H. (2020). Extreme rainfall in East Africa, October 2019–January 2020 and context under future climate change. *Weather*, 3(December 2019), 1–6. <https://doi.org/10.1002/wea.3824>
- Waithaka, M., Nelson, G. C., Thomas, T. S., & Kyotalimye, M. (2013). East African Agriculture

and Climate Change - Kenya Preview. In *East African Agriculture and Climate Change*.

- Waliser, D., Sperber, K., Hendon, H., Kim, D., Maloney, E., Wheeler, M., Weickmann, K., Zhang, C., Donner, L., Gottschalck, J., Higgins, W., Kang, I. S., Legler, D., Moncrieff, M., Schubert, S., Stern, W., Vitart, F., Wang, B., Wang, W., & Woolnough, S. (2009). MJO simulation diagnostics. *Journal of Climate*, 22(11), 3006–3030. <https://doi.org/10.1175/2008JCLI2731.1>
- Wang, B., Luo, X., Yang, Y. M., Sun, W., Cane, M. A., Cai, W., Yeh, S. W., & Liu, J. (2019). Historical change of El Niño properties sheds light on future changes of extreme El Niño. *Proceedings of the National Academy of Sciences of the United States of America*, 116(45), 22512–22517. <https://doi.org/10.1073/pnas.1911130116>
- Wanzala, M. A., Ficchi, A., Cloke, H. L., Stephens, E. M., Badjana, H. M., & Lavers, D. A. (2022). Assessment of global reanalysis precipitation for hydrological modelling in data-scarce regions: A case study of Kenya. *Journal of Hydrology: Regional Studies*, 41(May), 101105. <https://doi.org/10.1016/j.ejrh.2022.101105>
- Wanzala, M. A., Stephens, E. M., Cloke, H. L., & Ficchi, A. (2022). Hydrological model preselection with a filter sequence for the national flood forecasting system in Kenya. *Journal of Flood Risk Management*, May, 1–24. <https://doi.org/10.1111/jfr3.12846>
- Wenhaji Ndomeni, C., Cattani, E., Merino, A., & Levizzani, V. (2018). An observational study of the variability of East African rainfall with respect to sea surface temperature and soil moisture. *Quarterly Journal of the Royal Meteorological Society*, 144(August), 384–404. <https://doi.org/10.1002/qj.3255>
- Wheeler, M. C., & Hendon, H. H. (2004). An all-season real-time multivariate MJO index: Development of an index for monitoring and prediction. *Monthly Weather Review*, 132(8), 1917–1932. [https://doi.org/10.1175/1520-0493\(2004\)132<1917:AARMMI>2.0.CO;2](https://doi.org/10.1175/1520-0493(2004)132<1917:AARMMI>2.0.CO;2)
- Williams, A. P., & Funk, C. (2011). A westward extension of the warm pool leads to a westward extension of the Walker circulation, drying eastern Africa. *Climate Dynamics*, 37(11–12), 2417–2435. <https://doi.org/10.1007/s00382-010-0984-y>

- World Meteorological Organization (WMO). (2021). *WMO Guidelines on Multi-hazard Impact-based Forecast and Warning Services Part II: Putting Multi-hazard IBFWS into Practice* (Issue 1150). [https://library.wmo.int/?lvl=notice\\_display&id=21994](https://library.wmo.int/?lvl=notice_display&id=21994)
- Xiang, B., Zhao, M., Ming, Y., Yu, W., & Kang, S. M. (2018). Contrasting impacts of radiative forcing in the Southern Ocean versus southern tropics on ITCZ position and energy transport in one GFDL climate model. *Journal of Climate*, *31*(14), 5609–5628. <https://doi.org/10.1175/JCLI-D-17-0566.1>
- Yan, L., Du, Y., & Zhang, L. (2013). Southern ocean SST variability and its relationship with ENSO on inter-decadal time scales. *Journal of Ocean University of China*, *12*(2), 287–294. <https://doi.org/10.1007/s11802-013-2262-1>
- Yuan, D., Hu, X., Xu, P., Zhao, X., Masumoto, Y., & Han, W. (2018). The IOD-ENSO precursory teleconnection over the tropical Indo-Pacific Ocean: dynamics and long-term trends under global warming. *Journal of Oceanology and Limnology*, *36*(1), 4–19. <https://doi.org/10.1007/s00343-018-6252-4>
- Zsótér, E., Pappenberger, F., Smith, P., Emerton, R. E., Dutra, E., Wetterhall, F., Richardson, D., Bogner, K., & Balsamo, G. (2016). Building a multimodel flood prediction system with the TIGGE archive. *Journal of Hydrometeorology*, *17*(11), 2923–2940. <https://doi.org/10.1175/jhm-d-15-0130.1>